NATIONAL ADVISORY COMMITTEE FOR AERONAUTICS

TECHNICAL NOTE 2137

AN ANALYSIS OF BASE PRESSURE AT SUPERSONIC

VELOCITIES AND COMPARISON WITH EXPERIMENT

By Dean R. Chapman

Ames Aeronautical Laboratory
Moffett Field, Calif.

NACA

Washington

July 1950

NATIONAL ADVISORY COMMITTEE FOR AERONAUTICS

TECHNICAL NOTE 2137

AN ANALYSIS OF BASE PRESSURE AT SUPERSONIC

VELOCITIES AND COMPARISON WITH EXPERIMENT

By Dean R. Chapman

SUMMARY

In the first part of the investigation an analysis is made of base pressure in an inviscid fluid, both for two-dimensional and axially-symmetric flow. It is shown that for two-dimensional flow, and also for the flow over a body of revolution with a cylindrical sting attached to the base, there are an infinite number of possible solutions satisfying all necessary boundary conditions at any given free-stream Mach number. For the particular case of a body having no sting attached only one solution is possible in an inviscid flow, but it corresponds to zero base drag. Accordingly, it is concluded that a strictly inviscid-fluid theory cannot be satisfactory for practical applications.

Since the exact inviscid-fluid theory does not adequately describe the conditions of a real fluid flow, an approximate semi-empirical theory for base pressure in a viscous fluid is developed in a second part of the investigation. The semi-empirical theory is based partly on inviscid-flow calculations, and is restricted to airfoils and bodies without boat-tailing. In this theory an attempt is made to allow for the effects of Mach number, Reynolds number, profile shape, and type of boundary-layer flow. The results of some recent experimental measurements of base pressure in two-dimensional and axially-symmetric flow are presented for purposes of comparison. Some experimental results also are presented concerning the support interference effect of a cylindrical sting, and the interference effect of a reflected bow wave on measurements of base pressure in a supersonic wind tunnel.

INTRODUCTION

The present investigation is concerned with the pressure acting on the base of an object moving at a supersonic velocity. This problem is of considerable practical importance since in certain cases the base drag can amount to as much as two-thirds of the total drag of a body of revolution, and as much as 80 percent of the total drag of an airfoil.

In the past, numerous measurements of base pressure on bodies of revolution have been made both in supersonic wind tunnels and in free flight, but these experimental investigations have had no adequate theory to guide them. As a result, the present-day knowledge of base pressure is very limited and many inconsistencies appear in the existing experimental data.

Various hypotheses as to the fundamental mechanism which determines the base pressure in supersonic flow over bodies of revolution were advanced years ago by Lorenz, Gabeaud, and von Kármán. (See references 1, 2, and 3, respectively.) These hypotheses, however, do not appear to be adequate. The equations which result are unsatisfactory either for predicting the base pressure or for correlating experiments. Figure 1, which shows a comparison of these theories with average experimental values for projectiles, illustrates the relatively large discrepancies that are involved.

A semi-empirical theory of base pressure for bodies of revolution has been advanced recently by Cope in reference 4. In certain qualitative respects this theory is similar to the semi-empirical theory of the present report, though the two analyses were developed independently. In contradistinction to preceding investigations, the present analysis and the analysis of reference 4 attempt to include not only the effects of Mach number but also the effects of Reynolds number and type of boundary-layer flow, since experiments have shown these effects to be important. Cope evaluates the base pressure by equating the pressure in the wake, as calculated from the boundary-layer flow, to the pressure as calculated from the exterior flow. In calculating the pressure from the boundary-layer flow, however, numerous approximations and assumptions are necessarily made which, according to Cope, result in no more than a first approximation.

The primary purpose of the investigation described in the present report is to formulate a method which is of value for quantitative calculations of base pressure on airfoils and bodies without boat-tailing. The analysis is divided into two parts. Part I consists of a detailed study of the base pressure in two-dimensional and axially-symmetric inviscid flow. The purpose of part I is to develop an understanding of the problem in its simplest form, rather than to obtain results having immediate practical value. In part II a semi-empirical theory is formulated since the results of part I indicate that an inviscid-flow theory cannot possibly be satisfactory for quantitative calculations of a viscous flow. A comparison of the semi-empirical theory with experimental results is also presented in part II of the report.

Much of the present material was developed as part of a thesis submitted to the California Institute of Technology in 1948. Acknowledgement is made to H. W. Liepmann of the California Institute of Technology for his helpful discussions regarding the theoretical considerations, and to

A. C. Charters of the Ballistic Research Laboratories,for making available numerous unpublished spark photographs which were taken in the free-flight experiments of reference 5.

NOTATION

C_1, C_2 constants

d rod or support diameter

h base thickness (base diameter for axially-symmetric flow, trailing-edge thickness for two-dimensional flow)

k_l, k_t empirical constants

L length upstream of base (body length for axially-symmetric flow, airfoil chord for two-dimensional flow)

M Mach number

p pressure

P pressure coefficient referred to free-stream conditions

$$\left(\frac{p - p_\infty}{\frac{1}{2} \rho_\infty U_\infty^2} \right)$$

P_b' base pressure coefficient referred to conditions just ahead of the base $\left(\dfrac{p_b - p_1}{\frac{1}{2} \rho_1 U_1^2} \right)$

P_{bi} base pressure coefficient for maximum drag in inviscid flow

P_b^* value of P_b' obtained by extrapolating to zero boundary-layer thickness the curve of best linear variation of P_b' with δ_1

q dynamic pressure $\left(\frac{1}{2} \rho U^2 \right)$

R gas constant

Re Reynolds number based on the length L

r   radial distance from axis of symmetry to point in the flow

T   temperature

t   thickness of wake near the trailing shock wave

U   velocity

β   angle of boat-tailing at base

γ   ratio of specific heats (1.4 for air)

δ   boundary-layer thickness

ε   correction parameter to dynamic pressure, defined by equation (8)

ρ   density

Subscripts

1   conditions just ahead of base

∞   conditions in the free stream

b   conditions at base

o   stagnation conditions

I. BASE PRESSURE IN AN INVISCID FLUID

Throughout this part of the report the effects of viscosity are completely ignored and the flow field determined for an inviscid fluid wherein both the existence of a boundary layer and the mixing of dead air with fluid outside a free streamline are excluded from consideration. It is assumed throughout that a dead-air region of constant pressure exists just behind the base and is terminated by a single trailing shock wave. Only airfoils and bodies without boat-tailing are considered in the analysis. As will be seen later, the assumption of zero viscosity oversimplifies the actual conditions; the results so obtained, though of considerable help in understanding the flow characteristics, agree only qualitatively with experimental results.

Two—Dimensional Inviscid Flow

Semi—infinite two—dimensional profile.— In order to achieve the
greatest possible simplicity at the outset, the case of a semi—infinite
profile will be considered first. By this is meant a profile of constant
thickness which extends from the base to an infinite distance upstream
(fig. 2). The problem at hand is to determine the flow pattern in the
neighborhood of the base. Since the effects of viscosity are at present
ignored and only steady symmetrical flows are considered, the problem is
simply that of determining the flow over a two—dimensional, flat, hori-
zontal surface which has a step in it (fig. 3).

It is easy to construct a possible flow pattern which satisfies all.
necessary boundary conditions including the requirement of constant
pressure in the dead—air region. For example, suppose the free—stream
Mach number is 1.50 and some particular value of the base pressure coef-
ficient, say $P_b = -0.30$, is arbitrarily chosen. Since the base
pressure is prescribed, the initial angle of turning through the Prandtl-
Meyer expansion at B (fig. 3) is uniquely determined, and in this
particular case is equal to $12.4°$. The pressure, and hence the velocity
and Mach number, must be constant along the free streamline BC. For the
example under consideration, the Mach number along the free streamline is
easily calculated from the Prandtl—Meyer equations to be 1.92. For a
uniform two—dimensional flow over a convex corner, the pressure depends
only on the angle of inclination of a streamline, hence it follows that
BC is a straight line. The triangle BCE therefore bounds a region of
uniform flow having the same pressure as the dead—air region. As the
trailing shock wave (fig. 3) extends outward from E to infinity, inter-
ference from the expansion waves gradually decreases its strength until
it eventually becomes a Mach wave. That part of the shock wave from C
to E must deflect the flow through the same angle as the expansion waves
originally turned it ($12.4°$ for the particular example under considera-
tion). This deflection certainly is possible since the Mach number in
the triangle BCE is 1.92 which, according to the well—known shock—wave
equations, is capable of undergoing any deflection smaller than $21.5°$.
As the flow proceeds downstream from the trailing shock wave CEF, the
pressure approaches the free—stream static pressure, thus satisfying the
boundary condition at infinity.

It is evident that a possible flow pattern has been constructed
which satisfies all the prescribed requirements as well as the necessary
boundary conditions. This flow, however, certainly is not the only
possible one for the particular Mach number (1.50) under consideration,
since any negative value of P_b algebraically greater than -0.30 also
would have permitted a flow pattern to be constructed and still satisfy
all boundary conditions. This is not necessarily true, though, if
values of P_b algebraically less than -0.30 are chosen, as can be seen
by picturing the conditions that would result if the base pressure were

gradually decreased. The angle of turning through the Prandtl-Meyer expansion would increase and point C in figure 3 simultaneously would move toward the base. The base pressure can be decreased in this manner only until a condition is reached in which the shock wave at C turns the flow through the greatest angle possible for the particular local Mach number existing along the free streamline. The base pressure cannot be further reduced and still permit steady inviscid flow to exist. The flow pattern corresponding to this condition of a maximum-deflection shock wave can be considered as a "limiting" flow of all those possible. There are obviously an infinite number of possible flows for a given free-stream Mach number, but only one limiting flow.

The limiting value of the base pressure coefficient can be easily calculated as a function of the free-stream Mach number by reversing the procedure described above for constructing possible flow patterns. Thus, for a given value of the local Mach number along the free streamline a limiting flow pattern can be constructed by simply requiring that the angle of turning be equal to the maximum-deflection angle possible for a shock wave at that particular local Mach number. By use of the Prandtl-Meyer relations the appropriate value of the free-stream Mach number is then directly calculated from the angle of turning and the local Mach number along the free streamline. This process can be repeated for different values of the local Mach number along the free streamline and a curve drawn of the limiting base pressure coefficient as a function of Mach number. Such a curve is presented in figure 4. The shaded area represents all the possible values of the base pressure coefficient for two-dimensional inviscid flow. The upper boundary of the shaded area corresponds to the limiting flow condition for various free-stream Mach numbers.

There is no reason apriori to say that for a given M_∞ the limiting flow pattern represents that particular one which most nearly approximates the flow of a real fluid. The curve representing these limiting flow patterns can be considered simply as being the curve of maximum base drag (and hence maximum entropy increase) possible in an inviscid flow. This is the only interpretation that will be given to this curve for the time being. Since it is these limiting solutions which will be singled out later for further use, a special symbol P_{b_i} will be used to designate the base pressure coefficient of such flows. It is evident from a comparison of figures 1 and 4 that in the Mach number region shown the values of P_{b_i} for two-dimensional flow correspond to very high base drags, being almost as high as if a vacuum existed at the base. At Mach numbers greater than or equal to 6.0, the values of P_{b_i} exactly correspond to a vacuum at the base.

Axially–Symmetric Inviscid Flow

Semi—infinite axially—symmetric body.— In principle the same method of procedure can be used for inviscid axially—symmetric flow as was used for inviscid two—dimensional flow. The axially—symmetric flows, however, are somewhat more involved than the corresponding two—dimensional flows. For example, in axially—symmetric flow the expansion wavelets issuing from the corner of the base are not straight lines as they are in Prandtl—Meyer flow. Moreover, additional complications arise since the flow conditions upstream of the trailing shock wave do not depend solely on the inclination of the streamlines at a given point, but depend on the whole history of the flow upstream of the Mach lines passing through that point. As a consequence of these complications, the free streamline of constant pressure cannot be straight.

In order to construct possible flow patterns as was done in the two—dimensional case, the method of characteristics for axially—symmetric flow must be used and each flow pattern built up step by step. The details of the particular method employed are described in reference 6. By use of the characteristics method the inviscid flow field corre—sponding to a given value of the base pressure coefficient can be con—structed for any given value of the Mach number. The shape of the free streamline is, of course, determined by the condition that the pressure and the velocity must be constant along it. An example of such a con—struction for a free—stream Mach number of 1.5 is given in figure 5(a). In this particular case, the base pressure coefficient which has been chosen arbitrarily is –0.25. It is to be noted that there is a striking difference between the axially—symmetric case (fig. 5(a)) and the two—dimensional case (fig. 3). The inviscid flow pattern for the axially—symmetric case cannot be constructed all the way to the axis of symmetry, and still satisfy the prescribed boundary conditions. This is a conse—quence of the curvature of the free streamline and the fact that the Mach number along the free streamline in the case under consideration is 1.84, which, at the most, is capable of deflecting a streamline only $19.9°$ by a single shock wave. As is illustrated in figure 5(a), the angle of incli—nation of the free streamline for this example is already $19.9°$ at a value of $r/r_0 = 0.552$, where r is the radial distance from the axis and $r_0 = h/2$ is the radius of the base. Since the angle of inclination of the constant—pressure free streamline would continue to increase monoton—ically as the axis is approached, the flow pattern of figure 5(a) cannot be constructed farther than the point shown $(r/r_0 = 0.552)$ and still leave a provision for the flow to be deflected through a single shock wave and become parallel to the axis of symmetry. This phenomenon is not attribut—able to the particular combination of Mach number and base pressure selected for figure 5(a). In figures 5(b), 5(c), 5(d), 5(e), and 5(f), several other examples are presented which illustrate the flow for differ—ent values of Mach number and for different values of base pressure coef—ficient. In each case the free streamline has been terminated at the

point where the local angle of inclination is equal to the angle corresponding to the greatest possible deflection by a single shock wave. It is evident that none of these flow patterns could be constructed down to the axis of symmetry. Altogether, approximately 30 flow patterns were constructed by the characteristics method; in no case could the flow be constructed all the way to the axis. This phenomenon is discussed further in a later place.

The flow patterns built up by the method of characteristics should not be regarded as unrealistic simply because the flow cannot be constructed all the way to the axis. In a real fluid the flow outside the boundary layer is similar because the wake behind the body fills the region near the axis and prevents the outer flow from reaching the axis. This fact suggests that the axially-symmetric inviscid-flow patterns should be investigated further as they might bear some relation to actual flows if the displacement effect of the wake is accounted for.

The flow fields containing a free streamline not meeting the axis of symmetry can be considered as those that would exist in inviscid flow about a body of revolution which has an infinitely long cylindrical rod (or "sting") attached to the base. As an example, the flow of figure 5(a) would correspond to a body having a rod of diameter $d = 0.552h$ attached to the base. (See fig. 6.) With such a model the trailing shock wave turns the free streamline through the greatest deflection possible for the given local Mach number along the free streamline. The flow field is therefore the limiting flow field of all those possible for the given free-stream Mach number and the given ratio of d/h.

Just as in the case of the two-dimensional body, there are also an infinite number of possible flow patterns for the body of revolution with a rod attached. This is true because for a given configuration as many additional flow patterns as desired can be constructed by simply selecting the base pressure to be any pressure between the free-stream pressure and the pressure corresponding to the limiting flow. The limiting flow pattern is to be given the same physical significance for axially-symmetric flow as for two-dimensional flow; that is, the corresponding base pressure coefficient P_{b_i} represents the maximum base drag possible for an inviscid flow with a single trailing shock wave and a given ratio of d/h.

By choosing different values of the base pressure coefficient for a fixed Mach number, the inviscid solutions determined by the method of characteristics enable a plot of P_{b_i} against d/h to be made. This procedure has been carried out for Mach numbers of 1.25, 1.5, 2.0, 2.5, 3.0, and 4.0. The results are shown in figure 7. Each point on the curves in this figure represents one flow pattern constructed by the characteristics method. The values for $d/h=0$ correspond to the semi-infinite body without a rod attached. It is to be noted that for each curve in figure 7 the value of P_{b_i} extrapolates to zero as d/h

approaches zero. This means that the base pressure is equal to the free-stream static pressure, the free streamline is undeflected, and the base drag is zero. Hence, the limiting flow pattern and the infinity of possible inviscid flows for $0 < d/h < 1$ degenerate into a single trivial solution corresponding to zero base drag for $d/h=0$. In figure 7 the limiting values as d/h approaches 1.0 correspond to the previously treated case of two-dimensional flow. It can be seen that this must be the case by visualizing the limiting process as taking place with both d and h approaching infinity, but with the difference $(h-d)$ held constant. The configuration approached in this manner would be a two-dimensional step of height $(h-d)/2$, and the pressure coefficient approached would be the limiting base pressure coefficient for two-dimensional inviscid flow. On the other hand, if d/h is equal to unity (instead of approaching it from values always less than unity), then the corresponding configuration would be a semi-infinite body of revolution with a cylindrical rod of the same diameter attached to the base. Although no dead-air region exists in this case since the flow is everywhere uniform, the base pressure in the physical sense would be the static pressure at the junction of body and rod, and hence P_{b_i} would be zero.

The fact that $P_{b_i}=0$ for $d/h=0$ appears anomalous on first thought, particularly when one remembers that the coefficient P_{b_i} represents the maximum possible base drag that can exist for an inviscid flow of the type being considered. An explanation can be obtained from a consideration of the equations of motion since they are the basis for the method of characteristics. This explanation, however, is not essential for an understanding of the main conclusions regarding base pressure, and hence is presented as Appendix A. It is apparent from the curves in figure 7 that with any reasonable extrapolation (as indicated by dotted lines) the base drag of an axially-symmetric body in an inviscid fluid is, if not zero, so small that it cannot possibly agree with the drag values determined by experiments in a viscous fluid. This strongly suggests that viscous effects are essential in determining the base pressure.

Finite axially-symmetric body.— Due to the influence of the nose on any projectile-shaped body of revolution, such as the one sketched in figure 8(a), the Mach number and pressure on a portion of surface parallel to the free-stream direction are considerably different from their respective values M_∞ and p_∞ in the free stream. (This difference is virtually zero for such an element of surface on an airfoil, since the local conditions in two-dimensional flow depend only on the local surface inclination.) It is clear that, irrespective of this difference, the same difficulty for $d/h=0$ exists near the axis as in the case of the semi-infinite axially-symmetric body; the inviscid flow cannot meet the axis of symmetry. Hence the free streamline must eventually become parallel to the axis as it passes downstream, as illustrated in figure 8(b). Since the pressure at infinity is equal to the free-stream static pressure, and since the pressure is constant along the free streamline, it follows that the only possible base pressure in the strictly inviscid flow is again the

free-stream static pressure. For present purposes it is sufficient to
note that the pressure p_1 is ordinarily less than p_∞. This means that
there must be a weak shock wave at the corner of the base (fig. 8(b)).
The free streamline must then curve slightly as it trails downstream to
infinity, eventually becoming parallel to the axis.

The flow illustrated in figure 8(b) represents the solution for a
finite axially-symmetric body. The base drag is zero, but the flow
pattern is not what would precisely correspond to a trivial solution (in
the mathematical sense of the word), as is the case for the semi-infinite
body. Nevertheless, this particular solution for inviscid flow clearly
has no bearing on any flow that has as yet been encountered in experimental
investigations. Again it appears that viscosity must be the dominating
mechanism in determining the flow pattern in a real fluid.

Nonuniqueness of the Inviscid Base-Pressure Flows

The occurrence of more than one possible solution in two-dimensional
flow and also in axially-symmetric flow with a rod attached does not
represent a new occurrence in inviscid flow theory. A similar situation
occurs, for example, in airfoil theory for an inviscid, incompressible
fluid. As is well known, a satisfactory solution in this case has been
found in the use of the so-called Kutta condition. Of the infinite number
of possible solutions for the incompressible potential flow over an
airfoil at a given angle of attack, only one corresponds to a finite
velocity at the trailing edge. Use of the Kutta condition to select this
particular solution is a fairly straightforward process, and can be readily
justified on the basis of qualitative consideration of viscous effects near
the trailing edge. Consideration of viscous effects might also be expected
to lead to a unique solution in the case of the infinite number of solu-
tions for the base pressure.

Apart from the effects of viscosity several other considerations,
such as stability of the flow, also have been of importance in other unre-
lated problems when selecting a suitable inviscid flow solution from a
possible choice of more than one. As an example of this the inviscid
channel flow studied in reference 7 may be cited. For the present problem,
however, the preceding analysis of axially-symmetric inviscid flows points
toward viscous effects (rather than stability of inviscid flow) as being
the essential mechanism determining the base pressure.

Even if consideration is given only qualitatively to the effects of
viscosity, the base-pressure problem is relatively involved. These con-
siderations, which are discussed subsequently, indicate that it is the
viscous mixing of dead air and the outside flow which makes only one
solution possible for given Mach and Reynolds numbers. From an academic
viewpoint this resolves the difficulty of having an infinite number of
possible solutions to the inviscid-flow problem, but unfortunately greatly

complicates matters from a practical viewpoint since it means that a sat-
isfactory theory of base pressure must, in some way, allow for the effects
of viscosity.

II. A SEMI-EMPIRICAL THEORY FOR BASE PRESSURE IN A VISCOUS
FLUID AND COMPARISON WITH EXPERIMENTAL RESULTS

Qualitative Effects of Viscosity on the Base-Pressure Flow

Two-dimensional flow.— A sketch showing the qualitative flow char-
acteristics for the viscous-fluid flow in the region of the base is given
in figure 9. The flow starts with a Mach number M_1, pressure p_1, and
boundary-layer thickness δ_1. Because the base pressure is lower than
the pressure p_1, a small fan of expansion wavelets originates at point A.
The existence of a dead-air region in a small volume immediately behind the
base is a result of the separation at point B. As a consequence of the
formation of a dead-air region it can be deduced that the pressure along
the streamline BC is approximately constant. For the case of laminar
flow in the boundary layer transition begins somewhere between B and C,
and after passing through the region of the trailing shock wave the flow in
the wake becomes completely turbulent. The qualitative form of the
boundary-layer profiles at two stations between points B and C must take on
the same nature as those existing at the boundary of a supersonic jet
issuing into ambient air. Because of the viscosity of the fluid, the dead
air is induced into a slow circulatory motion in the directions indicated
by the small arrows in figure 9. The viscous mixing process causes the
boundary layer to thicken as it approaches point C.

With this qualitative picture of the flow processes in mind, a brief
description can be given as to how the base pressure arrives at its steady-
state equilibrium value. To fix conditions in mind, suppose a jet of air
is pumped from the body into the dead-air region and then is suddenly
stopped. At the instant the jet is turned off, point C is far downstream
of its equilibrium position. Due to the scavenging effect of the outside
flow on the mass of dead air, some of this dead air is removed, thus
causing the angle of turning at the corner to be increased and the pressure
of the dead-air region to be decreased. The larger angle of turning
increases the velocity outside the boundary layer, which in turn increases
the scavenging action, thereby again lowering the pressure and starting the
cycle over again. Thus, point C moves rapidly to a position as close to
the base as possible. There is, however, at least one important factor
which prevents point C from going as far toward the base as that point
which would roughly represent the limiting solution for inviscid flow. As
C moves toward the base, the pressure ratio of the trailing shock wave
increases, making it more difficult for the scavenged air and the low-
velocity air in the boundary layer to overcome the pressure rise of the

shock wave and flow downstream. The opposition of this effect to the ones mentioned previously would serve to establish equilibrium. Thus it appears that the qualitative effect of viscosity is such as to select and modify one solution from the infinite number that are possible in an inviscid flow.

Axially—symmetric flow.— Since figure 9 represents only the qualitative flow characteristics near the base, it may be thought of also as representing these characteristics for an axially—symmetric flow. Evidently the same general reasoning applies here as was used in the two—dimensional case. As compared to the two—dimensional case there is, however, an additional reason for further spreading of the streamlines in the boundary layer as the trailing shock wave is approached. Since the mean radius of a streamtube in the boundary layer continually decreases as the trailing shock wave is approached, additional spreading is brought about in order to keep the annular cross—sectional area of the streamtubes approximately constant.

Basis for Correlation of Experimental Data

Assumptions.— If it is assumed that the flow separates from the corner of the base and not from a position farther upstream, then for a given type of boundary—layer flow the principal variables of the problem are p_b, p_1, ρ_1, U_1, δ_1, h, and β, as illustrated in figure 9. The base thickness h would be the trailing—edge thickness in the case of two—dimensional flow, and would be the base diameter in the case of axially—symmetric flow. It is assumed that only the conditions immediately upstream of the base affect the base pressure. Hence, the base pressure coefficient $P_b{}'$ referred to conditions just upstream of the base depends only on the corresponding dimensionless variables,[1] and may be written as

$$P_b{}' \equiv \frac{p_b - p_1}{\frac{1}{2}\rho_1 U_1{}^2} = f\left(M_1, \frac{\delta_1}{h}, \beta\right) \tag{1}$$

Although such a relation may be of some help in correlating experimental measurements, the appearance of the angle of boat—tailing β makes further analysis very difficult. Accordingly, only profile shapes without boat—tailing ($\beta = 0$) are considered.

One consequence of the above equation is that a common basis for comparison can easily be made for different profile shapes, because at supersonic velocities the difference between M_1 and M_∞, and between

---

[1] If desired, the dimensionless variable p_b/p_1 could be used in place of $P_b{}'$. The variable $P_b{}'$ has been chosen for the present investigation since it is proportional to the base drag; whereas p_b/p_1 is not.

p_1 and p_∞ is practically independent of the viscosity of the fluid and dependent only on the profile shape. Equation (1) also implies that the effect of increasing the length upstream of the base L, while holding all other parameters constant, will be the same qualitatively as the effect of decreasing the Reynolds number of the flow, since both of these effects increase the boundary—layer thickness. It can be foreseen, therefore, that the ratio L/h and the Reynolds number (based on the length L) combine into a single parameter which depends only on the type of boundary—layer flow. The length L would be the airfoil chord for the case of two—dimensional flow, and the body length for the case of axially—symmetric flow.

If the boundary—layer flow is laminar, then from dimensional analysis and the classical considerations of the terms involved in the boundary—layer equations, it follows that

$$\delta_1 \sqrt{\frac{U_\infty}{\nu_\infty L}} = f \ (M_\infty, \ \text{profile shape})$$

Rewriting this equation,

$$\frac{\delta_1}{h} = \frac{L/h}{\sqrt{\dfrac{U_\infty L}{\nu_\infty}}} f \ (M_\infty, \ \text{profile shape}) = \frac{C_2}{\sqrt{Re}} \frac{L}{h}$$

where C_2 is a function of the Mach number and profile shape, but independent of viscosity. For a given L/h, variations in profile shape affect the boundary—layer thickness principally through the action of the pressure gradients set up by the particular profile contour. As a first approximation the effects of variations in pressure distribution on the thickness of the boundary layer just ahead of the base will be neglected, since these effects should be small compared to the effects of Reynolds number and L/h ratio. Within the limits of this simplification the above equation is applicable to any profile shape or length. Hence in correlating the data for laminar boundary—layer flow the parameter $L/(h\sqrt{Re})$ is used in the absence of direct measurements of δ_1/h.

In the case of turbulent flow a similar parameter can be obtained. By approximating the turbulent boundary—layer profile with a 1/7—power law, the ratio δ_1/h for low—speed flow turns out to be inversely proportional to the 1/5 power of the Reynolds number. (For example, see reference 8.) Using this result, the appropriate parameter in correlating base—pressure data for turbulent boundary—layer flow would be $L/[h(Re)^{1/5}]$.

The quantity determined by experimental measurements is the coefficient P_b rather than P_b'. Consequently, before it is ascertained whether equation (1) correlates the available experimental data, the relation between P_b' and P_b must be developed.

Relation between $P_b{}'$ and P_b.— As was pointed out earlier, the conditions ahead of the base (M_1 and p_1) differ considerably from free-stream conditions in an axially–symmetric flow, but do not differ by an appreciable amount in a two–dimensional flow over a profile without boat–tailing. By allowing for this difference, the coefficient $P_b{}'$ can be expressed in terms of the more familiar coefficient P_b and the pressure distribution on the profile by a single equation applicable to both types of flow. By definition,

$$P_b{}' = \frac{p_b - p_1}{\frac{1}{2}\rho_1 U_1{}^2} = \frac{q_\infty}{q_1} \left[\frac{(p_b - p_\infty) - (p_1 - p_\infty)}{q_\infty} \right] = \frac{q_\infty}{q_1}(P_b - P_1) \qquad (2)$$

where

$$P_b = \frac{p_b - p_\infty}{\frac{1}{2}\rho_\infty U^2}$$

and

$$P_1 = \frac{p_1 - p_\infty}{q_\infty}$$

The ratio q_1/q_∞ can be written as

$$\frac{q_1}{q_\infty} = \frac{\rho_1 U_1{}^2}{\rho_\infty U_\infty{}^2} = \frac{\rho_1}{\rho_0{}'} \frac{\rho_0{}'}{\rho_0} \frac{\rho_0}{\rho_\infty} \left(1 + 2\frac{\Delta U}{U_\infty} \right) \qquad (3)$$

In this and subsequent equations, powers higher than the first of quantities such as $\dfrac{\Delta U}{U_\infty} \equiv \dfrac{U_1 - U_\infty}{U_\infty}$ are small in comparison to unity, and are therefore neglected. In equation (3), ρ_0 and $\rho_0{}'$ represent the stagnation densities corresponding to conditions in the free stream and to conditions just ahead of the base, respectively. Designating $\Delta M \equiv M_1 - M_\infty$ and again considering only first–order terms, it follows that

$$\frac{\rho_1}{\rho_0{}'} \frac{\rho_0{}'}{\rho_0} \frac{\rho_0}{\rho_\infty} = \left(\frac{1 + \frac{\gamma-1}{2} M_1{}^2}{1 + \frac{\gamma-1}{2} M_\infty{}^2} \right)^{\frac{-1}{\gamma-1}} \left(1 - \frac{\Delta p_0}{p_0} \right) = 1 - \frac{M_\infty \Delta M}{1 + \frac{\gamma-1}{2} M_\infty{}^2} - \frac{\Delta p_0}{p_0} \qquad (4)$$

where Δp_0 is the loss in total pressure on passing through the nose shock wave, and may often be neglected. From the energy equation

$$\frac{\Delta U}{U_\infty} = \frac{U_1^2 - U_\infty^2}{2U_\infty^2} = \frac{c_p(T_\infty - T_1)}{U_\infty^2} = \frac{c_p T_\infty}{U_\infty^2}\left(1 - \frac{T_1}{T_0}\frac{T_0}{T_\infty}\right)$$

or, using $c_p = \gamma R/(\gamma-1)$ and $M = U/\sqrt{\gamma R T}$

$$\frac{\Delta U}{U_\infty} = \frac{1}{(\gamma-1)M_\infty^2}\left[1 - \left(\frac{1+\frac{\gamma-1}{2}M_\infty^2}{1+\frac{\gamma-1}{2}M_1^2}\right)\right] = \frac{\Delta M}{M_\infty\left(1+\frac{\gamma-1}{2}M_\infty^2\right)} \tag{5}$$

hence the combination of equations (3), (4), and (5) gives

$$\frac{q_1}{q_\infty} = 1 + \left(\frac{2}{M_\infty} - M_\infty\right)\frac{\Delta M}{1+\frac{\gamma-1}{2}M_\infty^2} - \frac{\Delta p_0}{p_0} \tag{6}$$

The pressure coefficient P_1 is related to ΔM and Δp_0 by

$$P_1 = \frac{p_1 - p_\infty}{\frac{\gamma}{2}p_\infty M_\infty^2} = \frac{2}{\gamma M_\infty^2}\left(\frac{p_1}{p_0'}\frac{p_0'}{p_0}\frac{p_0}{p_\infty} - 1\right) = \frac{2}{\gamma M_\infty^2}\left[\left(\frac{1+\frac{\gamma-1}{2}M_\infty^2}{1+\frac{\gamma-1}{2}M_1^2}\right)^{\frac{\gamma}{\gamma-1}}\left(1 - \frac{\Delta p_0}{p_0}\right) - 1\right]$$

$$= -\frac{2\Delta M}{M_\infty\left(1+\frac{\gamma-1}{2}M_\infty^2\right)} - \frac{2}{\gamma M_\infty^2}\frac{\Delta p_0}{p_0} \tag{7}$$

Substitution of equation (7) into equation (6) yields the relation

$$\frac{q_1}{q_\infty} \equiv 1 + \epsilon = 1 + \left(\frac{M_\infty^2}{2} - 1\right)P_1 - \frac{2}{\gamma M_\infty^2}\left(1 + \frac{\gamma-1}{2}M_\infty^2\right)\frac{\Delta p_0}{p_0} \tag{8}$$

Equation (2) for P_b in terms of P_b' and the pressure distribution is then

$$P_b = P_b'(1+\epsilon) + P_1 \tag{9}$$

where both ϵ and P_1 are usually small compared to unity.

In two-dimensional flow P_1 is virtually zero for profiles without boat-tailing (provided the profile is slender and the Mach number is not too high), but in an axially-symmetric flow under the same conditions it is not. For extreme body shapes, such as a conical-nosed projectile with very short cylindrical afterbody, the term P_1 can represent a substantial portion of the base drag. Moreover, for these relatively short bodies of revolution there is a considerable pressure variation outward along the Mach lines issuing from the corner of the base, and hence some approximate method of determining P_1 must be formulated which allows for this variation.

The method used herein to estimate P_1 is based on the following considerations: To fix ideas, it will suffice to consider a body such as is sketched in figure 8. The dotted lines in this sketch represent Mach lines. For present purposes these lines will be thought of as small pressure waves; those with positive tangents (e.g., DD') being members of the so-called first family, and those with negative tangents (e.g., D'A) being members of the so-called second family. Small pressure waves issuing from the body can affect the base pressure in several ways. For example, waves of the first family starting between D and E (fig. 8) reflect from the nose shock wave between D' and E', and then become members of the second family between D'A and E'G. These latter waves directly interact with the dead-air region. Other pressure waves of the first family, such as the one starting from F, affect the base pressure indirectly through an interaction effect on the second family of waves between D'A and E'G. (It is assumed that waves of the second family lying beyond E'G do not affect the base pressure.) The net effect of profile shape on base pressure of a finite body, therefore, will be determined approximately by the average strength of the second family of pressure waves as they meet the dead-air region behind the base. If a hypothetical cylindrical afterbody of diameter h were added to the base, then this second family of pressure waves would cause the pressure and Mach number along the hypothetical extended afterbody to differ from the corresponding free-stream conditions. This difference would be a measure of the coefficient P_1 and of the effect of profile shape on base pressure. Thus, P_1 may be thought of as a correction to P_b for the effects of profile shape, and can be determined approximately by the average pressure coefficient along a hypothetical cylindrical afterbody extending a length of about two diameters downstream of the base (the approximate length of dead-air region). Since P_1 is small compared to P_b, such approximate methods of evaluating it should suffice. For simplicity in the present investigation, P_1 is arbitrarily evaluated from the pressure coefficient on the hypothetical extended afterbody at a distance of one diameter from the base, rather than by evaluating it with some more complicated averaging process.

Experimental Data for Two–Dimensional Flow

At present the available experimental results on base pressure in two–
dimensional flow are rather limited, but they are sufficient to provide a
qualitative check on one particular result of the inviscid–flow calcula-
tions; this result concerns the essential difference, as indicated by the
inviscid–flow calculations, between the base pressure in two–dimensional
flow and in axially–symmetric flow. The absolute magnitude of the base
pressure coefficient for two–dimensional inviscid flow at a given Mach
number is represented by the limit of the axially–symmetric value as d/h
approaches unity in figure 7. For low and moderate supersonic Mach
numbers this limiting value is several times the value for axially–
symmetric flow, which, as will be seen later, is represented in figure 7
by a d/h ratio somewhere between 0.5 and 0.8. For high supersonic Mach
numbers the difference between the two types of flow, according to
figure 7, is small. These considerations which indicate that, except at
high supersonic Mach numbers, a pronounced difference should exist between
the base pressure in two–dimensional and axially–symmetric flow, are in
agreement with existing data. In reference 9, the wind–tunnel measure-
ments for two–dimensional flow over a wedge airfoil at a Mach number of
1.4 and a Reynolds number of 0.6 million indicate a value of –0.41 for the
base pressure coefficient. Measurements presented later for axially–
symmetric flow at the same Mach number and Reynolds number, however, indi-
cate values around –0.20. This large difference is in accord qualitatively
with the conclusions drawn from considerations based on the curves of
figure 7.

In order to make a preliminary evaluation of the Reynolds number
effect on base pressure in two–dimensional flow, some measurements have
been made on a constant–chord wing of finite span having a thick trailing
edge.[2] Because the ambient air near the wing tips can flow laterally
around the tip and into the low–pressure region behind the base, the data
cannot be considered as strictly representing two–dimensional flow.
Nevertheless, the ratio of span to base thickness (40) was sufficiently
large on the wing employed so that tip effects should not affect conclu-
sions concerning the qualitative influence of Reynolds number on base
pressure in two–dimensional flow. The results of base–pressure measure-
ments taken at a Mach number of 2.0 are shown in figure 10(a). It is
apparent that the base drag increases considerably as the Reynolds number
increases. Since the surfaces of the wings were smooth, and the highest
Reynolds number attained was 1.8 million, the data are representative of
the case of laminar flow in the boundary layer. A plot of these data
against the parameter $L/(h\sqrt{Re})$, which is proportional to the boundary-
layer thickness, is shown in figure 10(b). It is to be noted that in this

---

[2]These data were taken in the Ames 1– by 3–foot supersonic wind tunnel
No. 1 employing a wing of 9–inch span with a base–pressure orifice
located 1 inch outboard of the plane of symmetry.

form the data correlate fairly well to a straight line in the region
covered by the tests.

Experimental Data for Axially—Symmetric Flow

Fortunately, there are sufficient experimental data available for
axially—symmetric flow to make a fairly extensive correlation of P_b'
with the parameters $L/(h\sqrt{Re})$ and $L/[h(Re)^{1/5}]$, where h is now
the base diameter. Most of these data have been obtained from wind—tunnel
measurements on bodies of revolution mounted from the rear by a cylindrical
support. Accordingly, a knowledge of the possible support and wall inter-
ference effects is necessary for a satisfactory interpretation of the wind-
tunnel measurements. Some experimental data on support interference and
reflected bow-wave interference are presented in Appendix B. It will
suffice for the present purposes to state that the wind—tunnel measure-
ments were taken with a support sting of sufficient unobstructed length
so that no interference effect of support length is present in the data.
Likewise, no appreciable interference resulting from the reflected bow
wave is present in the data. As regards the effects of support diameter,
it is known from a relatively complete set of interference measurements
made by Edward W. Perkins of Ames Aeronautical Laboratory, part of which
is presented later, that the data taken at $M = 1.5$ are essentially free
of support interference. At the higher Mach numbers, however, a complete
set of support—diameter interference measurements was not made. Con-
sequently, some effect may be present in the data taken at $M = 2.0$ and
$M = 2.9$. For consistency, these data which may be affected to a small
extent by support—diameter interference have been taken with a fixed value
of 0.4 for the ratio of support diameter to base diameter. By comparing
the base pressure measured on various bodies tested with the same relative
support diameter, the effects of body shape can be deduced if it is assumed
that changes in nose shape do not produce significant changes in the sup-
port interference. This is believed to be a valid assumption for the body
and support dimensions used.

In reducing the experimental data for correlation the measurements
are first expressed in terms of conditions just ahead of the base. All
bodies of revolution used in the experimental investigations consisted of
either a cone—cylinder ($10°$ semiangle of cone) or an ogive—cylinder
(10—caliber ogival radius) combination. In order to determine the body—
shape correction (P_1) the pressure distribution over such combinations has
been calculated using the method of characteristics. Two typical pressure
distributions for a Mach number of 2.0 are shown in figure 11. For the
reasons explained earlier, the correction P_1 is determined by selecting
the value of the pressure coefficient existing on an extension of the
cylindrical afterbody at a location approximately one diameter downstream
of the base. The values of P_1 determined in this manner enable the
experimental data to be reduced to the form

$$P_b' = \frac{P_b - P_1}{1 + \epsilon} \tag{10}$$

The quantity P_b' should not depend on the body shape for a given Mach number approaching the base. For all but a few exceptional shapes, such as a simple cone without an afterbody, the Mach number approaching the base is sufficiently close to the free-stream Mach number to enable a direct comparison to be made between various body shapes. For these exceptional cases, which represent small values of the length-diameter ratio, an additional correction $\frac{\partial P_b}{\partial M}\,\Delta M$ is added to the right side of equation (10). Since even in an extreme case this latter correction is small compared to P_1, the derivative $\frac{\partial P_b}{\partial M}$ can be roughly estimated without affecting the final results appreciably. In the present tests this correction was made only for those bodies with a length-diameter ratio of 4 or less, since it amounted to only 4 percent of the measured data in the most extreme case and was negligible for the bodies with L/h greater than 4.

In attempting to correlate the available experiments it will be convenient to consider, separately, first the case of laminar flow in the boundary layer, and then the case of turbulent flow. The experiments representing the case of laminar boundary-layer flow were conducted on bodies of revolution with polished surfaces, and those representing turbulent flow were conducted on the same models with artificial roughness added in the form of a narrow transition strip. (See reference 10.) Although for simplicity the data are referred to simply as representing either laminar or turbulent flow, in a few cases the actual boundary layer may be in the transition state. It is to be noted that with smooth models transition (insofar as it affects base pressure) probably begins at Reynolds numbers of the order of 4 million. Likewise, with roughness added in order to obtain turbulent flow the artificial roughness may not bring about complete transition ahead of the base at Reynolds numbers less than about 2 million.

Laminar boundary-layer flow approaching base.— Wind-tunnel measurements of the base pressure for various bodies of revolution at a Mach number of 1.53 are shown in figure 12(a). These data, taken from reference 10, include the effect of variations in Reynolds number and body shape. The large effect of both Reynolds number and body shape is evident. Since the boundary-layer flow is laminar for these data, the extent to which correlation is achieved is most easily determined by plotting P_b' as a function of $L/(h\sqrt{Re})$. Figure 12(b) shows the data of figure 12(a) plotted in this form, from which it is evident that the experimental data correlate reasonably well to a single curve. The scatter of the various measurements about the mean line is attributed partly to the fact that the thickness and velocity profile of the boundary layer approaching the base, and hence the base pressure, are not strictly a function of the Reynolds number and length-diameter ratio alone.

The results of some measurements of the base pressure for various bodies with laminar boundary-layer flow at a Mach number of 2.0 are shown

in figure 13(a). These previously unpublished data were taken in the
Ames 1- by 3-foot supersonic wind tunnel No. 1 under conditions similar
to the tests at a Mach number of 1.53 reported in reference 10. The same
qualitative effects of body shape and Reynolds number as were observed at
a Mach number of 1.53 are evident from these data obtained at the higher
Mach number. Figure 13(b) shows the data of figure 13(a) plotted in the
form suitable for correlation according to the theoretical considerations.
Considering the wide variety of body shapes tested, it can be seen that
these data also correlate reasonably well to a single straight line.

Turbulent boundary—layer flow approaching base.— The results of
wind—tunnel measurements of base pressure on bodies of revolution at a
Mach number of 1.5 with turbulent boundary—layer flow approaching the
base are shown in figure 14(a). Also shown in this figure are the results
of free—flight measurements reported in reference 5. It is evident from
this figure that the effect of Reynolds number on base pressure is small;
whereas figure 12(a) shows that it is large in the case of laminar
boundary—layer flow. This is in qualitative accordance with theoretical
considerations since $(Re)^{1/5}$ occurs in the equations for turbulent flow
and $(Re)^{1/2}$ occurs for laminar flow.

The measured data of figure 14(a) are shown in figure 14(b) plotted
in the form suitable for purposes of correlating experimental data.
Since the body—shape correction (P_1) is independent of viscous effects,
the same corrections have been used for the case of turbulent flow as
were used for laminar flow. It may be seen from figure 14(b) that the
data correlate fairly well to a straight line.

Some experimental data for turbulent boundary—layer flow at a Mach
number of 2.0 are shown in figure 15(a) and the plot of $P_b{'}$ against
$L/[h(Re)^{1/5}]$ is shown in figure 15(b). The curves in these figures show
the same characteristic of relatively constant base pressure as was noted
above for turbulent boundary—layer flow at a Mach number of 1.5. Again,
there is a reasonably good correlation of these data, as is evident from
figure 15(b).

Formulation of Semi—Empirical Theory

Since the experimental data correlate fairly well to straight lines
in figures 10(b), 12(b), 13(b), 14(b), and 15(b), a simple semi—empirical
theory for profile shapes without boat—tailing can easily be formulated
which is in accordance with the measured data. In so doing there are two
principal assumptions that are made:

1. The base pressure coefficient $P_b{'}$ depends only on the type of
boundary—layer flow, the Mach number M_1, and the dimensionless boundary—
layer thickness δ_1/h which exists just upstream of the base.

2. At a given Mach number the difference $(P_b* - P_b')$, due to the effects of viscosity, is proportional to the dimensionless boundary-layer thickness δ_1/h.

It is clear that the equations which result from these two assumptions are in agreement with the base-pressure measurements presented. In view of assumption (2) and equation (9) relating P_b' to P_b, the equations for the base pressure coefficient are

$$P_b = P_b* \left(1 - \frac{k_l}{\sqrt{Re}} \frac{L}{h} \right) (1+\epsilon) + P_1 \qquad (11)$$

for laminar boundary-layer flow, and

$$P_b = P_b* \left(1 - \frac{k_t}{(Re)^{1/5}} \frac{L}{h} \right) (1+\epsilon) + P_1 \qquad (12)$$

for turbulent boundary-layer flow. It is to be noted that for a given type of boundary-layer flow these semi-empirical equations provide no information as to the dependence of P_b* and k_l (or k_t) on Mach number. Insofar as the semi-empirical analysis is concerned these quantities are to be evaluated by experiments, and within this limitation the above equation can be said to satisfactorily correlate the experimental data. To what extent these equations will satisfactorily correlate data for conditions existing at very high Mach and Reynolds numbers is a question that can only be answered by future experimental results.

As regards the numerical values of P_b*, k_l, and k_t, certain conclusions can be drawn from the existing data. From the slope of the lines in figures 12(b) and 13(b) the approximate value of k_l at a Mach number of 1.53 is 44, and at 2.0 it is 66. Thus, these data indicate a dependence of k_l on Mach number. It is interesting that for turbulent boundary-layer flow the slope of the curves in figures 14(b) and 15(b) is small and hence k_t could be neglected without serious loss of accuracy, at least for the range covered by the present tests.

Comparison of Experimental Results With the Inviscid-Flow Calculations

Since the quantity P_b* is independent of the Reynolds number, some correlation (possibly only qualitative) might be expected between the experimental values of P_b* and the inviscid-flow calculations, provided allowance is made for the displacement effect of the wake near the trailing shock wave. As long as the wake thickness is well defined (reasonably steady wake) a simple and plausible method of estimating P_b* would be to

evaluate the base pressure coefficient for maximum drag in an inviscid
flow wherein an equivalent solid object replaced the wake. Such an object
would have no effect in inviscid two-dimensional flow but would have a
pronounced effect in axially-symmetric flow. If in axially-symmetric flow
a rod of diameter d is considered to replace the wake of diameter t,
the resulting maximum drag in inviscid flow would be the same as calculated
in part I where the corresponding base pressure coefficient was designated
by P_{b_i}. (See fig. 7.) Thus an estimate for the variation of P_b^* with
Mach number in axially-symmetric flow would be

$$P_b^* \approx P_{b_i} \quad \text{for} \quad \frac{d}{h} = \frac{t}{h} \tag{13}$$

and in two-dimensional flow it would be

$$P_b^* \approx P_{b_i} \tag{14}$$

In making a comparison with experiments where the Reynolds number is essen-
tially constant, this relation is tantamount to implying proportionality
between P_b and P_{b_i}. Since a fluctuating wake presumably cannot be
replaced by a rod without essentially altering the flow conditions near the
base, the above equations cannot be expected under such conditions to yield
anything more than the right order of magnitude.

Some information on the thickness and steadiness of the wake has been
obtained from an examination of numerous spark photographs taken of projec-
tiles in free flight.[3] Typical spark photographs are shown in figure 16,
and the results of measuring the wake thickness on a large number of simi-
lar photographs are shown in figure 17. Figure 16(a) represents the case
of laminar flow in the boundary layer at a free-stream Mach number of 1.73.
Under these conditions the wake thickness appears to be reasonably well
defined, although the trailing shock wave is not well defined near the wake.
Figures 16(b) and 16(c) indicate that for turbulent boundary-layer flow on
bodies of revolution the trailing shock wave and the wake are not very
steady at Mach numbers below about 2. Thus it is not surprising that, as
will be seen later, equation (13) is in poor agreement with measurements
for turbulent boundary-layer flow at Mach numbers below about 2. At higher
Mach numbers the trailing shock wave and the wake become more clearly
defined (figs. 16(d) and 16(e)), but the accuracy of equation (13) in this
region cannot as yet be tested because of insufficient experimental data.

A comparison between inviscid-flow calculations and experimental values
of P_b^* is more direct for airfoils than for bodies of revolution since the

[3]These shadowgraphs were made available through the courtesy of the
Ballistic Research Laboratories, Aberdeen, Md.

wake thickness presumably need not be accounted for in two-dimensional flow. The value of $P_b{}^*$ as determined from the finite-span wing data in figure 10(b) is -0.30. This is fairly close to the limiting pressure coefficient (P_{b_i}) for two-dimensional flow, which is -0.33 for a Mach number of 2.0. (See fig. 4.) Definite conclusions as to the significance of this agreement, however, will have to await the results of measurements on airfoils at other Mach numbers, and on airfoils with turbulent flow in the boundary layer.

For laminar flow on bodies of revolution at Mach numbers of 1.5 and 2.0, the wake thickness (t/h) from figure 17 is 0.55 and 0.49, respectively. From figure 7, the corresponding values of P_{b_i} are -0.25 and -0.29, respectively. On the other hand, the values of $P_b{}^*$ determined from the intercepts of the extrapolated lines in figures 12(b) and 13(b) are -0.24 and -0.20, respectively. Hence, although the inviscid-flow calculations may provide a reasonable approximation for two-dimensional flow near $M = 2.0$, and for axially-symmetric flow near $M = 1.5$, there is a serious discrepancy with the experimental results for axially-symmetric flow at $M = 2.0$. This large discrepancy indicates that the simple relation given by equation (13) which attempts to connect $P_b{}^*$ with the inviscid calculations is not always a satisfactory approximation. The good agreement obtained in two of the three cases may be entirely fortuitous. Additional experiments are needed to clarify this point.

The fact that the inviscid-flow calculations agree qualitatively, though not quantitatively, with experimental results can be seen by a comparison with measurements of the base pressure at various Mach numbers but with an essentially constant Reynolds number. Figure 18 shows some experimental free-flight data of reference 5 together with the corresponding wind-tunnel data of the present investigation.[4] These experimental data are for turbulent flow in the boundary layer. In this figure the ordinate of the curve labeled "equation (13)" is proportional to the value of the limiting pressure coefficient P_{b_i} determined at each Mach number in the manner indicated by equation (13). It is apparent that the curve based on the calculations of P_{b_i} for inviscid flow gives the right order of magnitude for the base pressure coefficient, but does not give good quantitative agreement. As an incidental point, it may be noted that the wind-tunnel and free-flight measurements shown in this figure agree quite well at all Mach numbers.

<div align="center">

Variation of Base Pressure With Reynolds
Number for Natural Transition

</div>

Since the base pressure is different for laminar and turbulent boundary-layer flow approaching the base, it is of interest to examine

---

[4] In several cases wind-tunnel measurements were made in more than one facility. For example, the three experimental points in figure 18 representing the wind-tunnel data at Mach numbers near 1.5 represent measurements with three different nozzles.

the results of measurements in the intermediate range of Reynolds number
where the transition "point" moves from a position downstream of the base
to a position upstream of the base. Figure 19 shows the results of some
base-pressure measurements at a Mach number of 2.0 on a body of revolution
in the Reynolds number range from 0.4 million to 10 million. At Reynolds
numbers below about 2 million, where the boundary-layer flow is laminar,
the base pressure coefficient depends to a great extent on the Reynolds
number, as was noted earlier. In the Reynolds number range from 4 to
6 million, where the transition point moves ahead of the base, the base
pressure again is sensitive to changes in the Reynolds number (and pre-
sumably also to other factors affecting transition such as surface
roughness, free-stream turbulence, and rate of heat transfer). At the
higher Reynolds numbers where a turbulent boundary layer exists for some
distance ahead of the base, the base pressure is not sensitive to changes
in the Reynolds number.

From the viewpoint of reliably extrapolating small-scale measurements,
it is encouraging that the base pressure coefficient for turbulent boundary-
layer flow is not sensitive to changes in the Reynolds number. At a Mach
number of 2.0 this insensitivity is evident from a comparison of the data
for the model with an L/h of 5 in figures 15(a) and 19. At a Reynolds
number of 2×10^6, where turbulent flow is attained on the models by using
artificial roughness, the base pressure coefficient does not differ by
more than 3 or 4 percent from the value at a Reynolds number of 1×10^7,
where turbulent flow is attained without such an artifice. At a Mach num-
ber of 1.5 the measurements indicate this same characteristic, as can be
seen from the data given in figure 20. These data at the somewhat lower
Mach number do not show any appreciable dependence on Reynolds number
within the range from 2×10^6 to 1.6×10^7. It is interesting that the
free-flight data of Hill and Alpher (reference 11) also show no significant
effect of Reynolds number within the range from 2×10^7 to 1×10^8. These
latter data, however, give a widely different value for the base pressure.
It is evident from figure 20 that the base pressures measured in refer-
ence 11 differ from the values of reference 5 and the present wind-tunnel
tests because of some factor other than differences in Reynolds number.
The possible effects of support interference in the present wind-tunnel
tests would not appear to contribute any appreciable amount to this dis-
crepancy for two reasons. First, good agreement is obtained at all Mach
numbers between the present wind-tunnel tests and the free-flight firings
of reference 5; and second, the measurements of support interference as
described in Appendix B indicate that for the support dimensions used
($d/h = 0.25$ and $d/h = 0.40$ in fig. 20) these effects are an order of
magnitude smaller than the observed discrepancies. Since the models of
reference 11 were equipped with tail fins of sufficient size so that their
presence at moderate supersonic Mach numbers might be expected to lower
considerably the pressure approaching the base (algebraically lower the
effective P_1), it would appear that the observed discrepancy is attribu-
table to the effect of tail fins on base pressure.

CONCLUDING REMARKS

The simplest approach to an analysis of base pressure for supersonic flow is that of considering the flow of an inviscid fluid. Although such an approach has produced many useful theories when applied to other aerodynamic problems, it produces results of very limited value when applied to the present problem. The inviscid-fluid theory indicates that the only possible base pressure for a body of revolution without a rod attached to the base is the free-stream static pressure. Moreover, this simple theory also indicates that for two dimensional flows, as well as axially-symmetric flows with a rod attached to the base, there are an infinite number of possible solutions for a given body shape and Mach number.

The first of the above-mentioned shortcomings of inviscid theory can be remedied by allowing qualitatively for the existence of a wake, since by so doing the high-velocity streamlines are displaced from the axis of symmetry and a base drag other than zero can be obtained. The second shortcoming, of having an infinite number of possible solutions from which to choose, is not easily remedied. In particular, the comparison between the inviscid-flow calculations and experiment has shown that if the limiting flow pattern (maximum drag possible) at each Mach number is singled out from the infinity of possible inviscid-flow solutions, then the characteristics of base pressure observed thus far can be explained, but only qualitatively. Thus, the experimental finding that an increase in support diameter behind a body of revolution can considerably decrease the base pressure is explained by an interpretation of the behavior in an inviscid-fluid flow. Also, the experimental result of a much lower base pressure in two-dimensional flow (at moderate supersonic Mach numbers) than in axially-symmetric flow is satisfactorily explained by the inviscid-flow calculations. As regards quantitative results, though, the calculations based on the maximum drag possible in inviscid flow do not agree with the observed effects for turbulent boundary-layer flow, and agree only in certain cases with the observed effects for laminar boundary-layer flow.

In an attempt to formulate a more accurate quantitative analysis a semi-empirical theory has been developed. The available experimental data correlate reasonably well to straight lines when the base pressure coefficient, corrected for the effects of body shape, is plotted as a function of a parameter which is approximately proportional to the boundary-layer thickness. As a result of this correlation several general conclusions can be drawn. One such conclusion is that the variation of base pressure with Reynolds number is small at high Reynolds numbers where the boundary layer approaching the base is turbulent, but is large at low Reynolds numbers where the boundary layer is laminar. Another conclusion is that the effects of body shape are independent of the type of boundary-layer flow, and can be adequately explained on the basis of inviscid calculations.

In order to develop a thorough understanding of the behavior of base pressure in supersonic flow, further experimental and theoretical investigations are required. At present, experimental results are especially needed as regards the base pressure in two-dimensional flow, even at low supersonic Mach numbers. The effect of tail fins on bodies of revolution appears to be relatively large, and hence should be investigated thoroughly. Experiments conducted at high supersonic Mach numbers are also needed, both for two-dimensional flow and for axially-symmetric flow.

Ames Aeronautical Laboratory,
        National Advisory Committee for Aeronautics,
                Moffett Field, Calif., May 11, 1950.

APPENDIX A

AXIALLY—SYMMETRIC FLOWS CONVERGING TOWARD THE AXIS

The rather anomalous result obtained when applying the method of characteristics to base—pressure flows can be clarified by examining the basic equations of motion on which the method of characteristics is based. The differential equation for the velocity potential φ of an inviscid axially—symmetric compressible flow is (see reference 6, for example)

$$\left(1 - \frac{\varphi_x^2}{a^2}\right)\varphi_{xx} - 2\frac{\varphi_x\varphi_r}{a^2}\varphi_{xr} + \left(1 - \frac{\varphi_r^2}{a^2}\right)\varphi_{rr} + \frac{\varphi_r}{r} = 0 \qquad (A1)$$

where a is the local velocity of sound, x is the coordinate measured parallel to the direction of the undisturbed stream, and r is the radial coordinate. If a transformation is made to a new system (ξ, η) of curvilinear coordinates, where ξ and η are distances measured along the two Mach lines issuing from a point, then the equation of motion for the velocity potential becomes simply (the details of the algebra involved in making this transformation may be found in reference 6),

$$\frac{\partial^2 \varphi}{\partial\xi\partial\eta} = \frac{\sin^2 \alpha}{r} \frac{\partial\varphi}{\partial r} \qquad (A2)$$

where α is the local Mach angle. It is to be noted that the new variables have the simple physical significance that lines of constant ξ and η are the Mach lines of the flow. The derivative of the velocity potential in any given direction is the projection of the velocity vector along that direction, and the order of differentiation in equation (A2) can be interchanged

$$\frac{\partial\varphi}{\partial\xi} = p \qquad \frac{\partial\varphi}{\partial\eta} = q \qquad (A3)$$

and

$$\frac{\partial\varphi}{\partial r} = v = w \sin \theta$$

where w is the velocity vector inclined at an angle θ with respect to the axis. It follows from equation (A2) that along Mach lines

$$dp = \frac{\sin^2 \alpha}{r} v \, d\eta \qquad dq = \frac{\sin^2 \alpha}{r} v \, d\xi \qquad (A4)$$

Thus, dp is the increment in the projection of the velocity vector along the ξ direction when passing a distance $d\eta$ in the physical plane along the η direction, and dq is the increment in the projection of the velocity vector in the η direction when passing a distance $d\xi$ along the ξ direction. Equations (A4) are the fundamental equations used in the step-by-step construction of a supersonic flow by Sauer's or Frankl's method of characteristics.

The reasons for the singular behavior as the flow approaches the axis of symmetry can now be explained with the help of equations (A4). Suppose a series of steps were laid off in the physical plane in the manner indicated by the sketch shown in figure 21(a). The small increments $(d\xi$ and $d\eta)$ along the Mach lines are laid off such that they are always small compared to the distance from the axis r and also such that for all steps $d\xi/r$ and $d\eta/r$ are always very nearly equal to a constant, say C. It is to be noted that if such a flow converging to the axis is possible, then there would be an infinite number of such steps along the streamline AB in figure 21(a).

Now consider the increments in the hodograph plane corresponding to those laid off in the physical plane (fig. 21(a)). Figure 21(b) illustrates the way, according to equations (A3) and (A4), in which the increments must be laid off in the velocity plane. Points having the same number in figures 21(a) and 21(b) represent the same point in the flow. Let the smallest average Mach angle along the steps in the physical plane be α_m, and the smallest vertical-velocity component be v_m, then for all steps along AB

$$|dp| > |v_m\ C\ \sin^2 \alpha_m| = \text{constant}$$

and

$$|dq| > |v_m\ C\ \sin^2 \alpha_m| = \text{constant}$$

This means that every increment in the hodograph plane is greater than a constant value. This value cannot be zero unless points 1 and 3 are identical, which would represent the exceptional case of a "reversed" conical flow. On passing from point A to point B there are, however, an infinite number of such increments. They must be laid out along the arc of a circle in the hodograph plane since AB is a streamline of constant pressure. Hence, before reaching point B the inclination angle of the velocity vector must be greater than $46°$ (approximate maximum deflection angle through a single shock wave for $\gamma = 1.4$). Because this situation obviously prevents a shock wave from being fitted into the flow, there results a contradiction to the assumption that the over-all flow is possible. It appears, therefore, that these flows are not always possible.

The preceding discussion, though not a mathematically rigorous exposition, points out the reason why the inclination angle θ of a free streamline can increase at an excessive rate as the axis is approached. The source of the trouble is inherently associated with the last term in the equation of motion (A1), since it has r in the denominator and a nonvanishing factor in the numerator. The appearance of r in the denominator of this equation stems entirely from the continuity equation. This leads to a qualitative explanation of the observed behavior near the axis of the inviscid flows. Consider the changes that must occur on going from point 1 to point 3 in the physical plane (fig. 21(a)). If the flow were two-dimensional, then the free streamline would be straight and θ_1 would equal θ_3, thereby preserving the cross-sectional area between two adjacent streamlines on passing from 1 to 3. The term involving $1/r$ does not occur for plane flow and no difficulties arise. In the axially-symmetric case, the fundamental condition is again that the cross-sectional area of an annular streamtube must be preserved, since w_1 is equal to w_3. This means that for purely geometric reasons the streamlines bounding the annular streamtube must spread apart as the axis is approached. In order to have the pressure at point 3 equal to that at point 1, the free streamline curves toward the axis, permitting the bounding streamlines to spread, thereby allowing the continuity equation to be satisfied. Because of the $1/r$ term in the continuity equation, the curvature rapidly increases as the axis is approached. Hence, before the axis is reached, the inclination of the free streamline exceeds the largest value which any oblique shock wave can possibly overcome.

APPENDIX B

WIND—TUNNEL SUPPORT INTERFERENCE AND REFLECTED
BOW—WAVE INTERFERENCE

When a body of revolution is tested in a wind tunnel it is usually supported from the rear by a cylindrical rod. As a result the measured values of base pressure may be considerably affected, for one thing, by the presence of the support. Support interference on base pressure is a complicated function of the diameter of support rod, the unobstructed length of support rod, the Mach number, and the Reynolds number. If, as is the case for the experiments referred to herein, the support length is much greater than the base diameter, then the only appreciable interference must arise from the "diameter effect" of the rod. From theoretical considerations certain inferences can be drawn regarding the resulting support—diameter interference on base pressure.

For a fixed Mach and Reynolds number, an increase in the support diameter brings about two different effects. First, the wake thickness is increased, thereby making it possible for lower base pressures to exist. (See fig. 7.) A second effect resulting from an increase in support diameter is that the appropriate dimensionless boundary—layer thickness $\delta_1/(h-d)$ is increased, thereby tending to increase the base pressure. The two effects, therefore, oppose each other. For values of d/h near unity the second effect must predominate; whereas for small values of d/h the first effect would (on the basis of fig. 7) be expected to predominate, especially at low supersonic Mach numbers.

Before comparing these theoretical considerations with experimental measurements of the effect of variations in d/h, it will be advantageous to first consider the effects of having only a finite length of unobstructed support rod. To examine this effect, base—pressure measurements have been taken with a constant value of d/h, but with various lengths of unobstructed support. In these experiments the model was located at a fixed position in the test section so as to eliminate possible effects of axial pressure gradients along the test section. The results from $M = 2.0$ and 2.9 are illustrated by the curves in figure 22, which show, for $d/h = 0.3$, no change in base pressure if the support length is greater than about 3 base diameters. Since support lengths of over 4 body diameters have been used in all subsequent tests, it is concluded that any interference in the wind—tunnel measurements of base pressure at $M = 2.0$ and 2.9 is not attributable to effects of support length.

The results of base—pressure measurements for various support diameters with laminar boundary—layer flow are shown in figure 23(a). The

data for a Mach number of 1.5 (which were taken by Edward W. Perkins in 1946) show the expected increase, and then eventual decrease in base drag as the support diameter is progressively increased. At a Mach number of 2.9 the data show a monotonic decrease in base drag as the support diameter is increased. Schlieren photographs show that the wake thickness t/h varies from approximately 0.5 to 1.0 as d/h varies from 0 to 1.0. Consequently, it turns out that the behavior of the three curves in figure 23(a) is qualitatively the same as would be indicated if equation (13) were used to estimate $P_b{}^*$. (It is to be remembered that t/h is the "effective" d/h of fig. 7.)

The corresponding results for turbulent boundary–layer flow are shown in figure 23(b). At Mach numbers of 1.5 and 2.0 these data show the same trends as for laminar boundary–layer flow, but at a Mach number of 2.9 the trend is not the same. At Mach numbers near 3, and possibly higher, it appears that the relative importance of the two above–mentioned effects of increasing d/h depends on the condition of the boundary–layer flow.

It may be noted from figure 23(a) that there is one point corresponding to $d/h = 0$ on the curve representing laminar flow at a Mach number of 1.5. This point, which was determined from the measurements using a side support gives the same value for the base pressure as exists for a support with a d/h ratio of about 0.3. At all the other Mach numbers, where special interference measurements were not made, the base pressure was measured with a constant value of 0.4 for the ratio d/h. From the curves in figure 23(a) it may be inferred that, at least for Reynolds numbers of the order of 4 million, the base–pressure data for laminar flow are not significantly affected by support interference.

Unfortunately, an investigation of support interference for turbulent boundary–layer flow has not been made using a side support. Definite quantitative statements about the possible effects of support interference in the turbulent–flow data (figs. 14, 15, 18, 19, and 20) cannot be made at present. Evidence that the combined effects of support and wall interference are not large, however, is given by the good agreement obtained at all Mach numbers between the free–flight firings of reference 5 and the various wind–tunnel measurements (figs. 14, 15, 18, and 20).

A possible source of wall interference arises from the reflection of a bow wave from the side walls, and the eventual intersection and interaction with the wake at some downstream position. This interaction for $M = 2.0$ and $M = 2.9$ occurs at a position varying from 7 to 22 base diameters downstream of the base. Since the large disturbance caused by the balance housing has no measurable effect at distance of 3 base diameters from the base (see fig. 22), there is no reason to expect that the base–pressure measurements at $M = 2.0$ and $M = 2.9$ might be affected by reflections of bow waves from the tunnel side walls. At a Mach number of 1.5, however, the downstream position of interaction is closer; it varies

from approximately 2.7 base diameters for the model with an L/h of 7, to 5.4 base diameters for the model with an L/h ratio of 4.3. In view of the possible interference from reflected bow waves at low supersonic Mach numbers, a special investigation was made prior to the tests of reference 10 to determine the magnitude of this effect. The results, taken at a Mach number of 1.53,[5] are presented here as they aid in evaluating the accuracy of the wind-tunnel measurements of base pressure.

Figure 24 illustrates the test setup employed in evaluating the effect of a reflected bow wave on base pressure. Because of symmetry the two outer dummy models caused two shock waves, similar to reflected bow waves, to interact with the wake behind the base of the center model (on which the base pressure was measured). By varying the distance between the dummy models of the test setup, the position of interaction was readily changed. The strength of the bow wave on the models employed (6-caliber ogival radius) in this special investigation varied from approximately two to eight times the strength of the bow wave on the various models for which base-pressure data are presented.

Schlieren photographs of the flow for two different positions of interaction, and two different Reynolds numbers, are given in figure 25. The distance x, from the base to the position of interaction, is equal to 2.5h in both figures 25(b) and 25(c). This particular position simulates the closest position to the base of the interaction of reflected waves in the present tests. The corresponding base-pressure measurements[6] without and with the interference wave present are illustrated in figure 26 by the circle and triangle symbols, respectively. The data show no appreciable effect on base pressure of the shock wave which simulates a reflected bow wave. If a reflected bow wave comes too close to the base, however, then large interference effects are possible, as illustrated by the square symbols in figure 26, and the corresponding schlieren photographs in figure 25(d). Except for purposes of illustrating this effect, base-pressure measurements were, of course, not taken under these latter conditions of important interference from reflected waves. Since the simulated reflection waves of the models used in this special investigation were several times stronger than the bow waves on the models for which the base pressure was measured, it is clear from figure 26 that the wind-tunnel measurements presented are not appreciably affected by interference of a reflected bow wave.

---

[5]This Mach number differs somewhat from that of more recent tests (at M=1.50) since the earlier tests were conducted in 1946 at a time when the 1- by 3-foot supersonic wind tunnel was temporarily equipped with a set of fixed nozzle blocks instead of the flexible plates now employed.

[6]These data fall slightly below other data presented herein because of the very small amount of boat-tailing on the models used in this special investigation.

REFERENCES

1. Lorenz, H.: Der Geschosswiderstand. Physikalische Zeitschrift, vol. 18, 1917, p. 209; vol. 29, 1928, p. 437.

2. Gabeaud: Sur la resistance de l'air aux vitesses ballistiques. Comptes Rendus de l'Academie des Sciences, vol. 192, 1931, p. 1630.

3. von Kármán, Th., and Moore, N. B.: The Resistance of Slender Bodies Moving at Supersonic Velocities. Trans. of ASME, vol. 54, 1932, p. 303.

4. Cope, W. F.: The Effect of Reynolds Number on the Base Pressure of Projectiles, NPL Rep. Eng. Div. 63/44, Jan. 1945.

5. Charters, A. C., and Turetsky, R. A.: Determination of Base Pressure from Free-Flight Data. Aberdeen Ballistic Res. Lab., Rep. 653, Mar. 1948.

6. Sauer, R.: Theoretische Einführung in die Gasdynamik. Julius Springer, Berlin, 1943. (Reprinted by J. W. Edwards Bros., Inc., Ann Arbor, Mich.)

7. Kantrowitz, A.: The Formation and Stability of Normal Shock Waves in Channel Flows. NACA TN 1225, 1947.

8. Prandtl, L., and Tietjens, O. G.: Applied Hydro and Aeromechanics. McGraw-Hill Book Co., Inc., New York, 1934, p. 76.

9. Valensi, J., and Pruden, F. W.: Some Observations on Sharp Nosed Profiles at Supersonic Speed. British A.R.C., Fluid Motion Sub-Committee, 10607 (FM1108), May 1947.

10. Chapman, Dean R., and Perkins, Edward W.: Experimental Investigation of the Effects of Viscosity on the Drag of Bodies of Revolution at a Mach number of 1.5. NACA RM A7A31a, 1947.

11. Hill, Freeman K., and Alpher, Ralph A.: Base Pressures at Supersonic Velocities. Jour. Aero. Sci., vol. 16, no. 3, Mar. 1949, pp. 153 – 160.
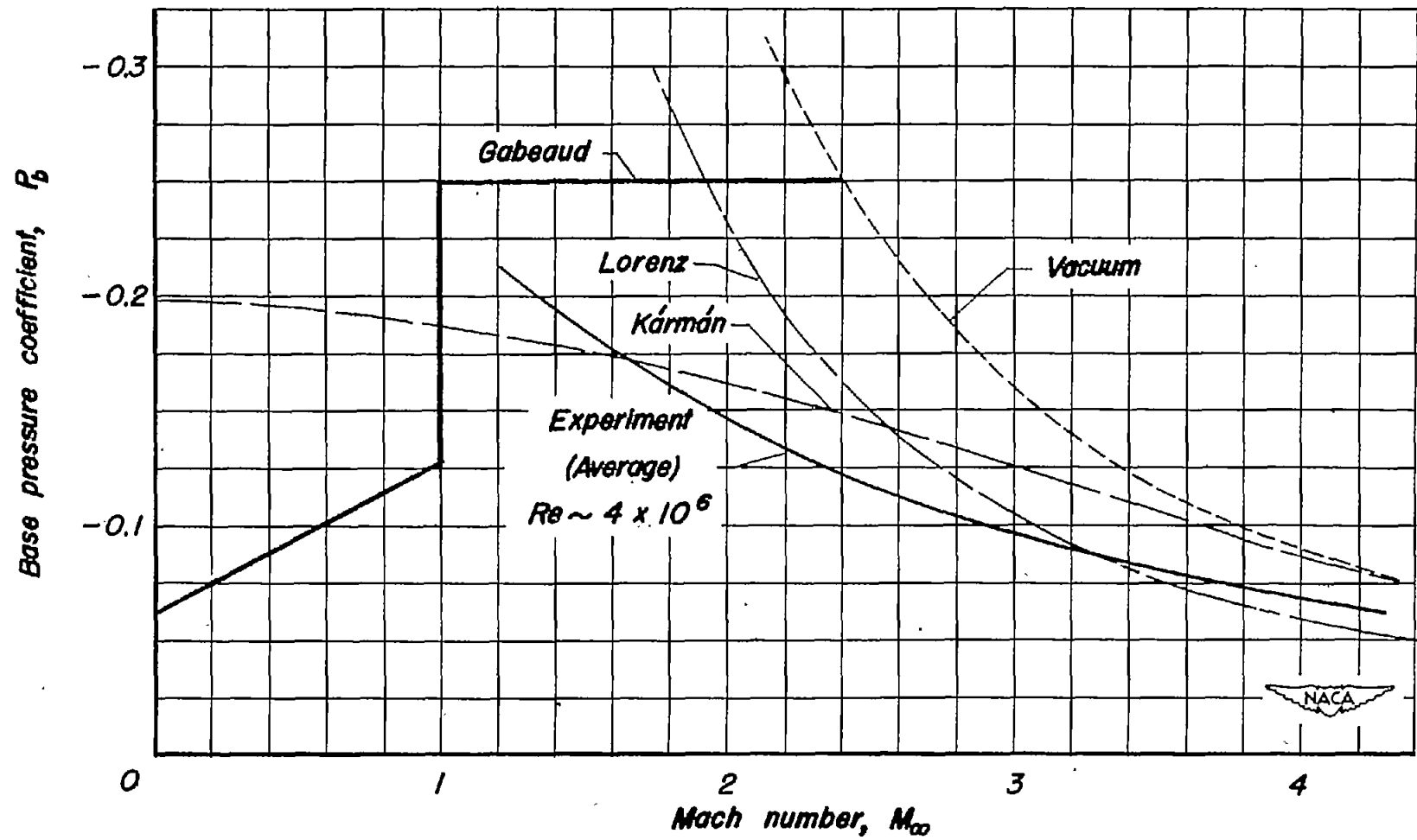
Figure I.—Comparison of the existing theories of base pressure.
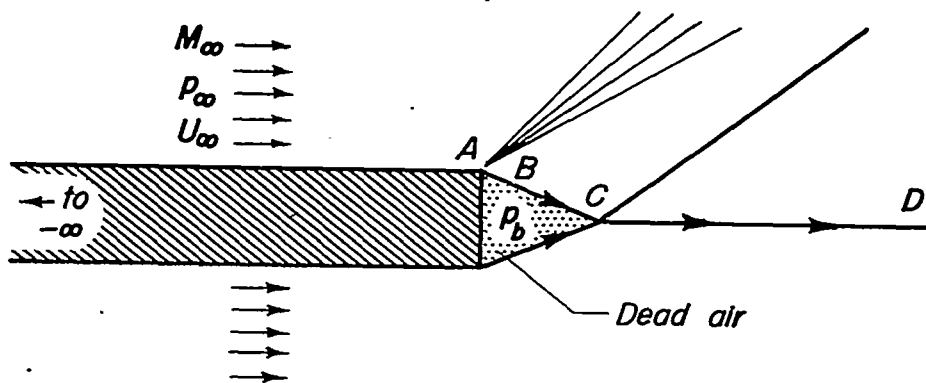
Figure 2. —Semi-infinite profile.
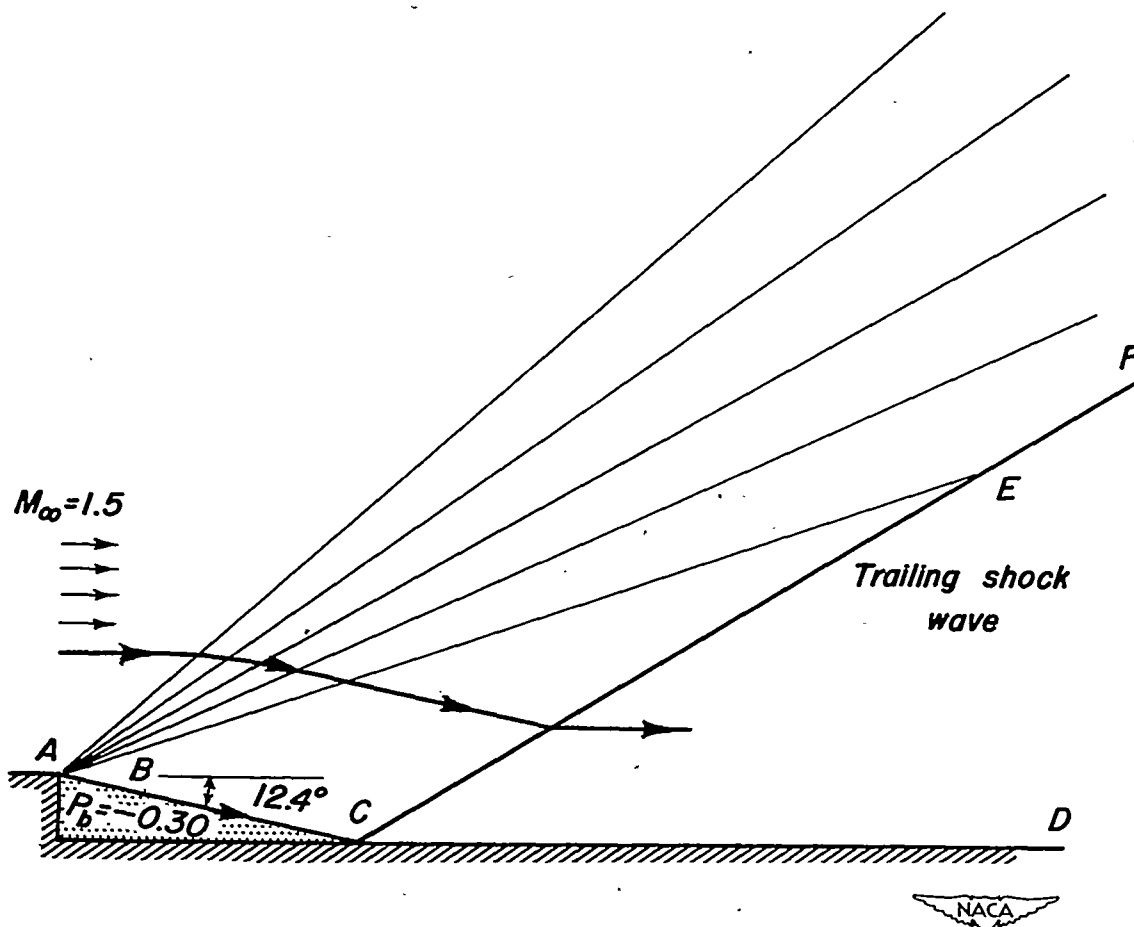
Figure 3. —Example of inviscid flow over a two-dimensional profile.
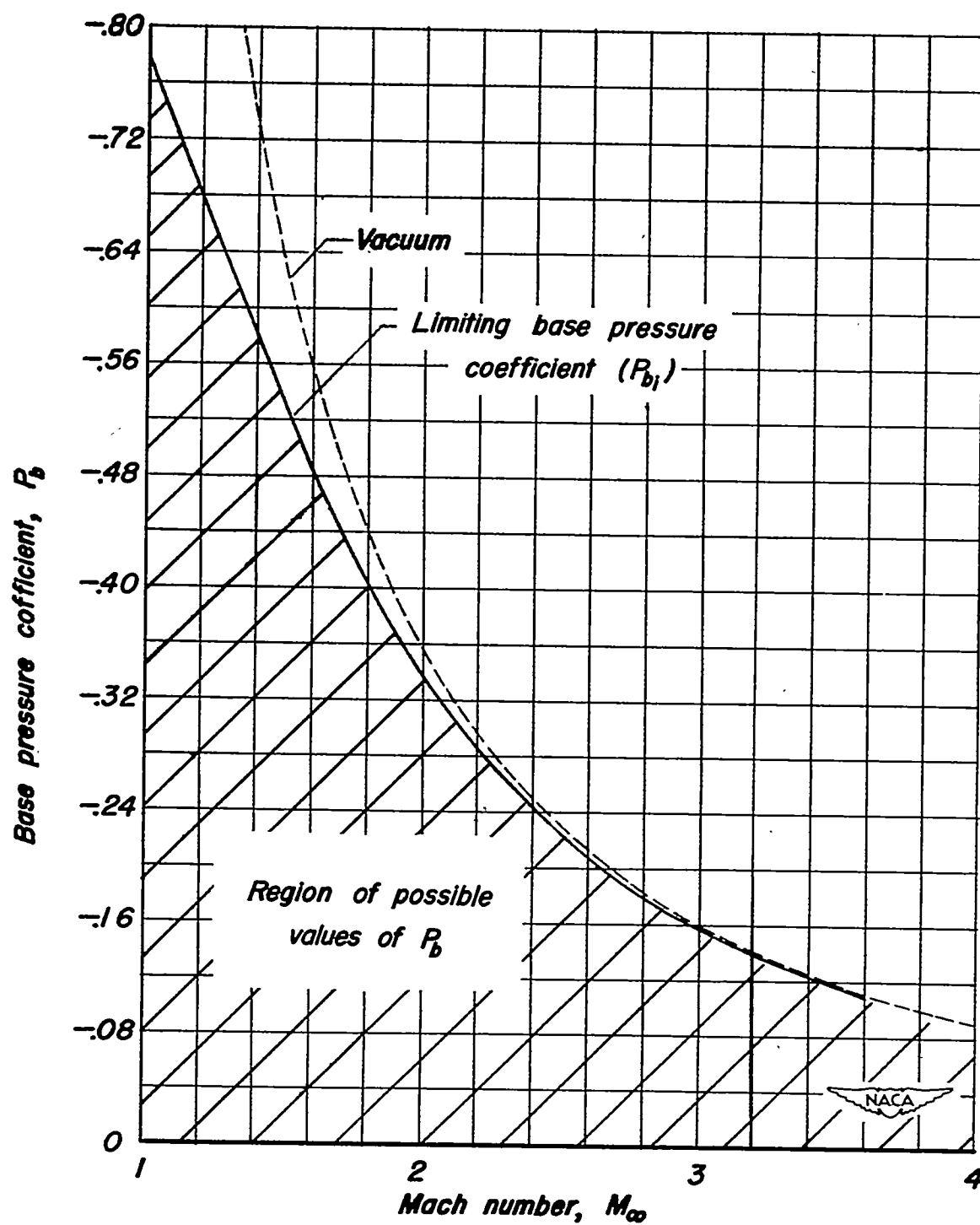
Figure 4.—Base pressure for two-dimensional inviscid flow.

Uniform flow

$M_\infty = 1.5$

Free streamline $M = 1.84$

19.9°

$r_0 = \dfrac{h}{2}$

Dead-air space

Uniform pressure P_b

$r = 0.552\, r_0$

Axis of symmetry

$(a)\ M_\infty = 1.5;\quad P_b = -0.25.$
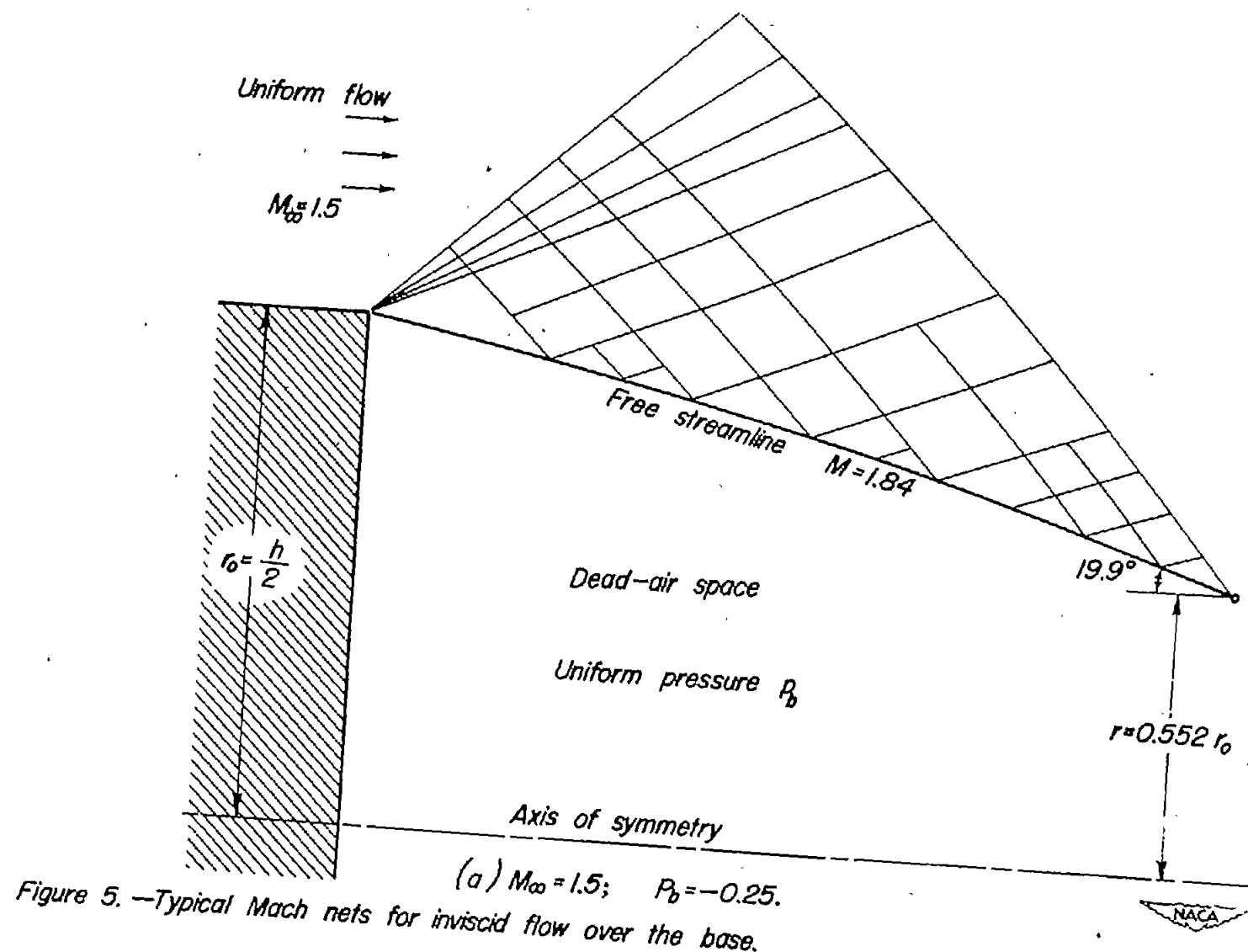
Figure 5. —Typical Mach nets for inviscid flow over the base.

(b) $M_\infty = 2.5$; $P_b = -0.215$.

Figure 5. — Continued.

M=3.70

37.5°

0.275 r_0
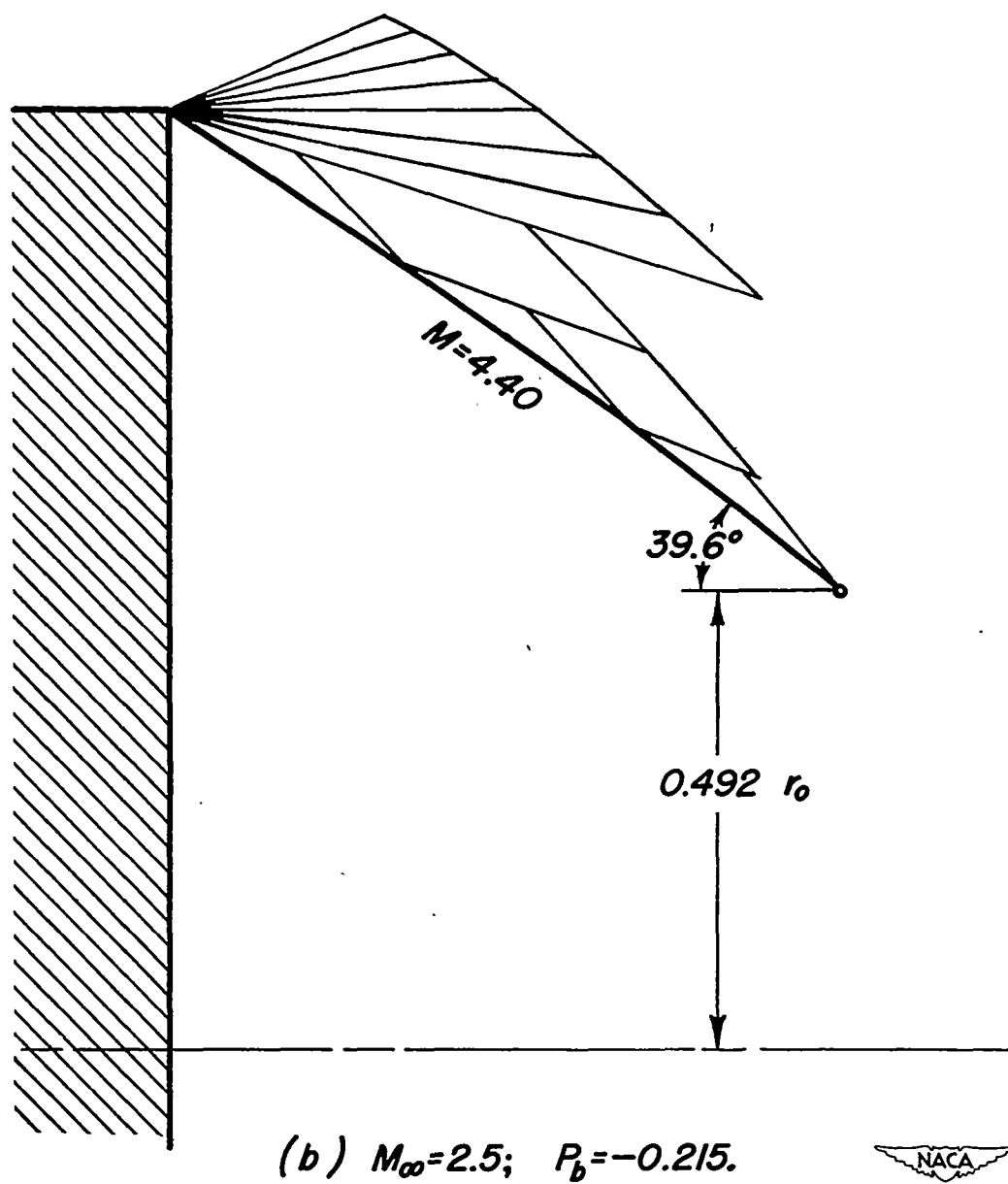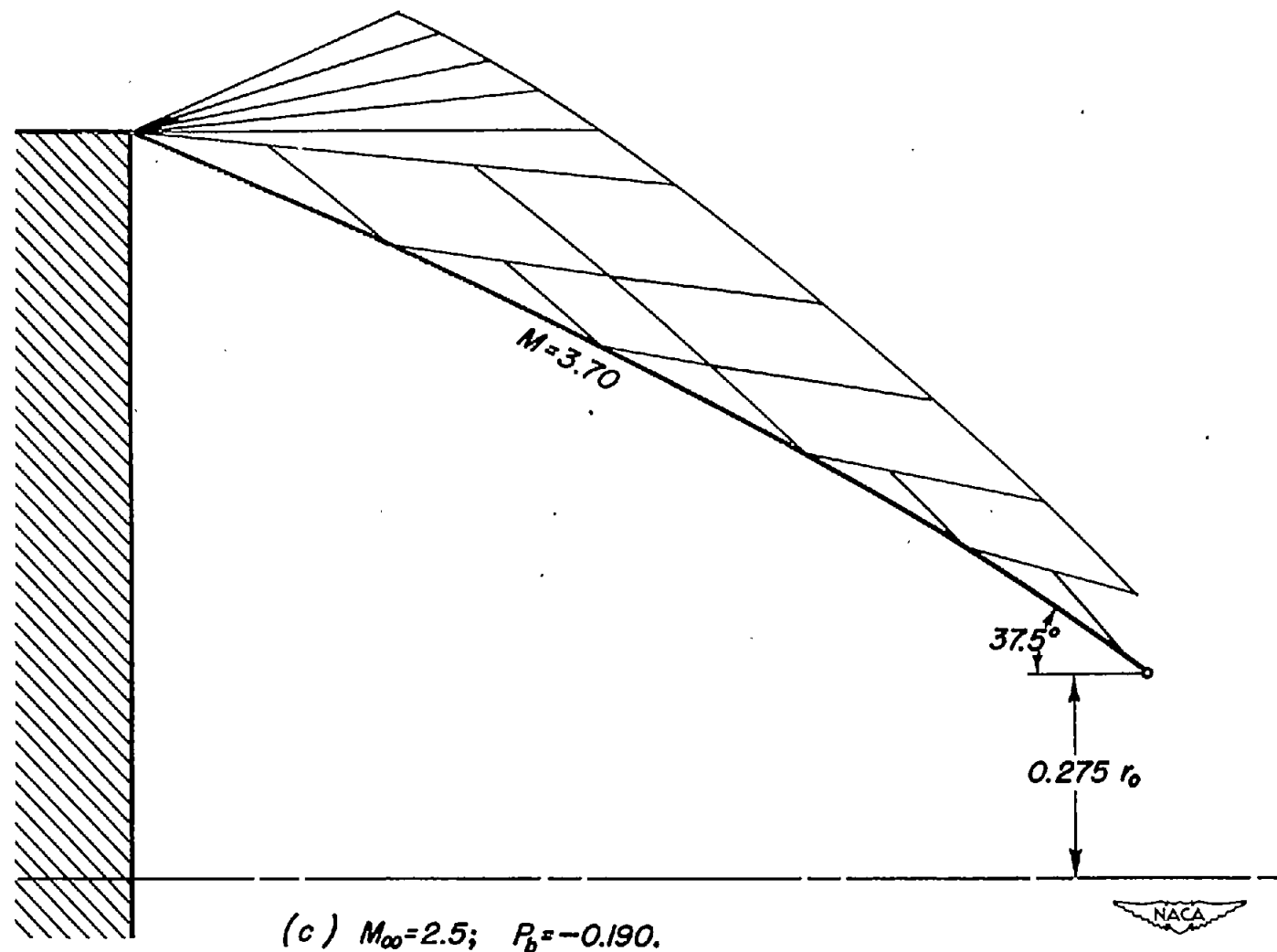
(c) $M_\infty = 2.5$; $P_b = -0.190$.

Figure 5. — Continued.

$M=3.40$

$34.9°$

$0.226 r_o$

(d) $M_\infty=2.5$; $P_b=-0.170$.

Figure 5. —Continued.

$M=2.93$

$33.5°$

$0.107 r_0$
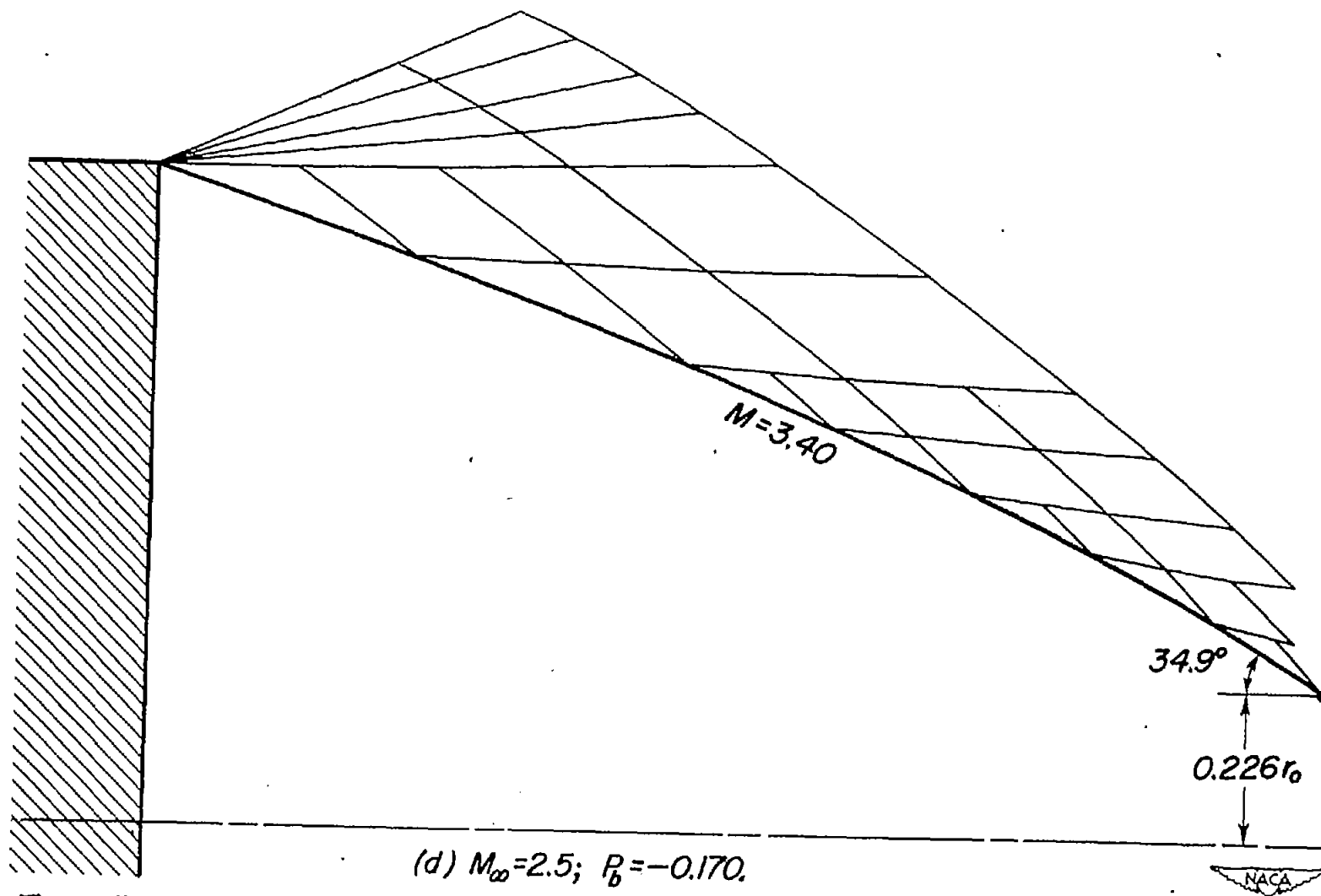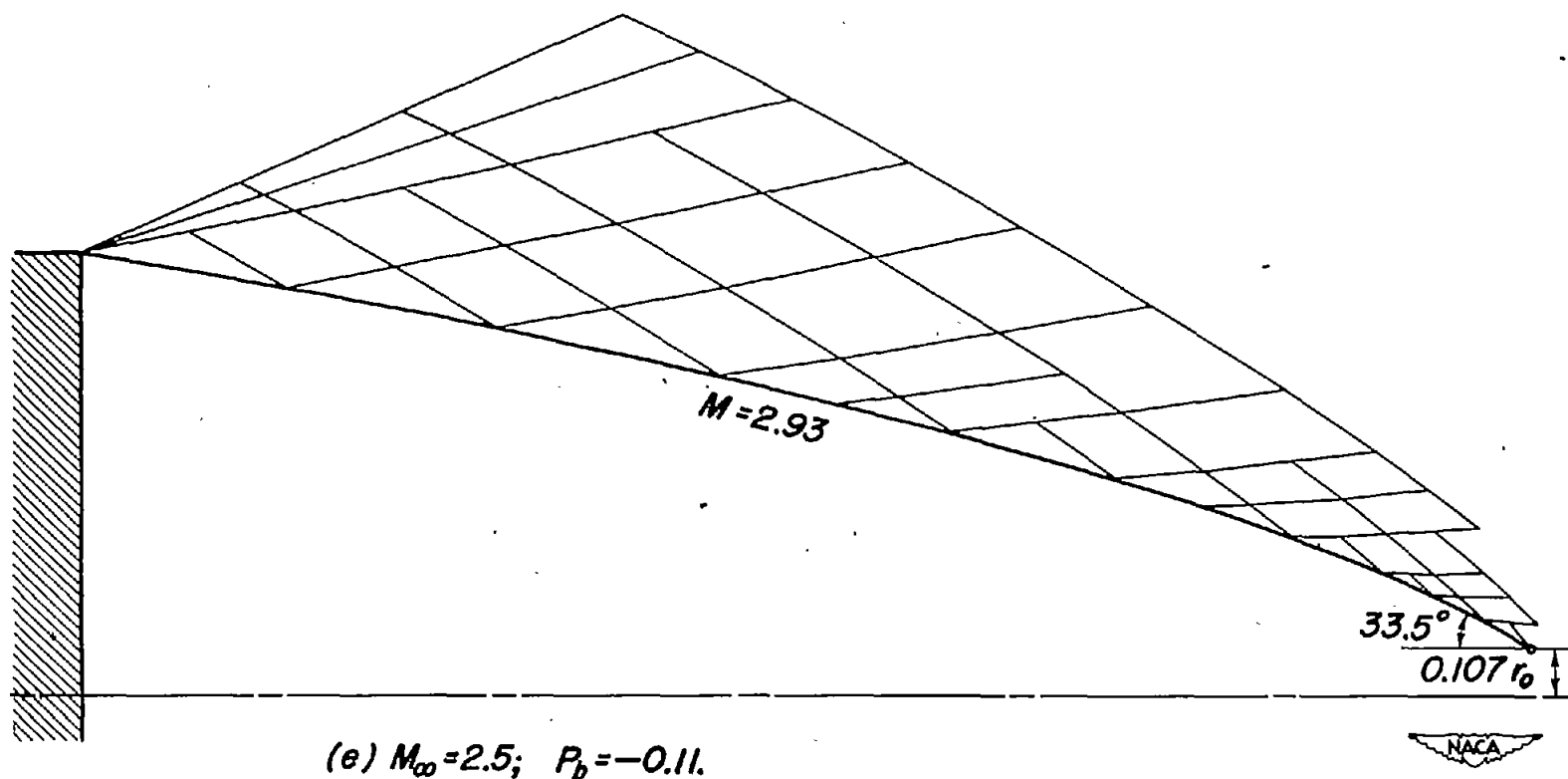
(e) $M_\infty = 2.5$; $P_b = -0.11$.

Figure 5. —Continued.

(f) $M_{\infty} = 4.0$; $P_b = -0.0806$.
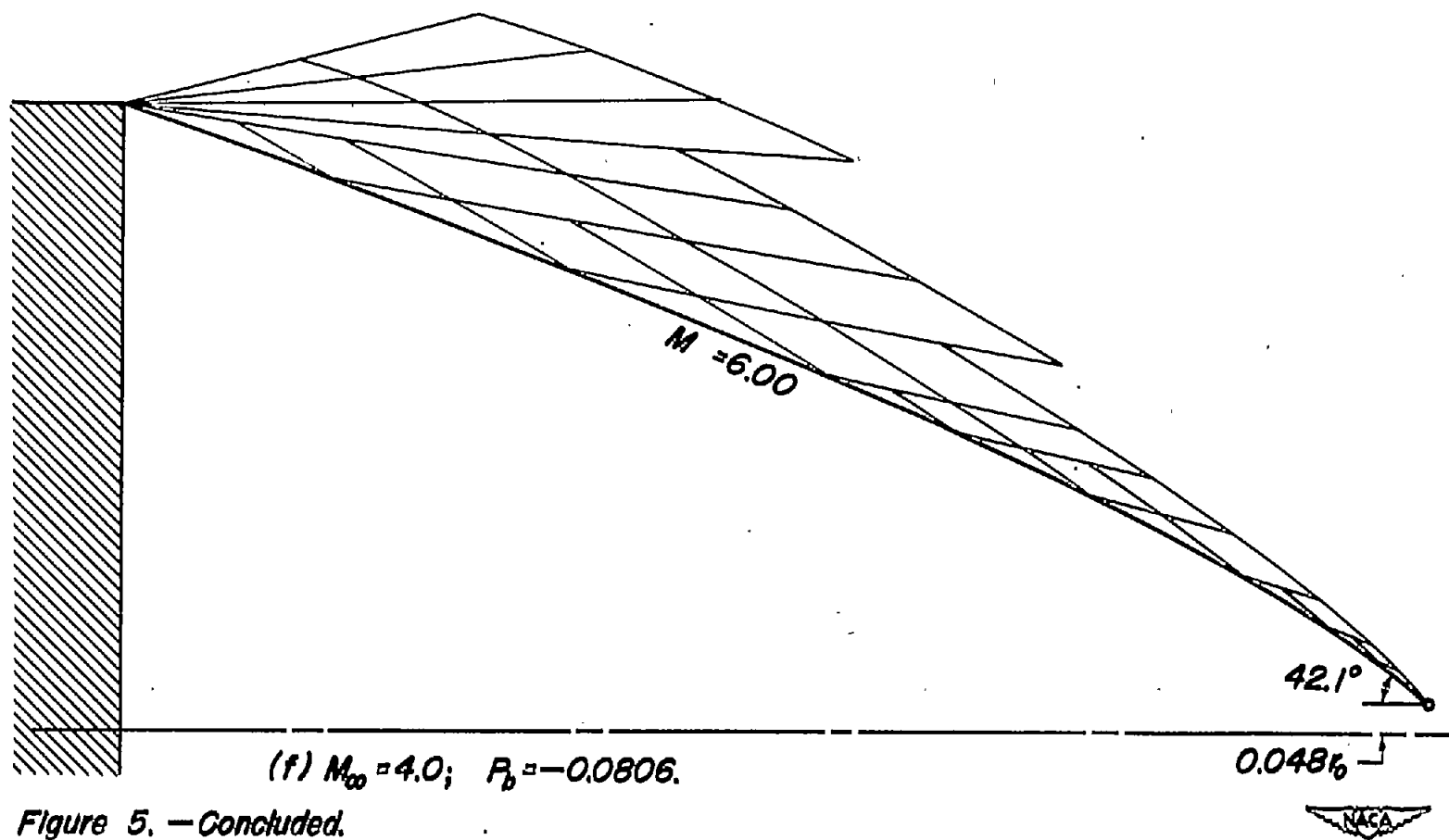
Figure 5. — Concluded.
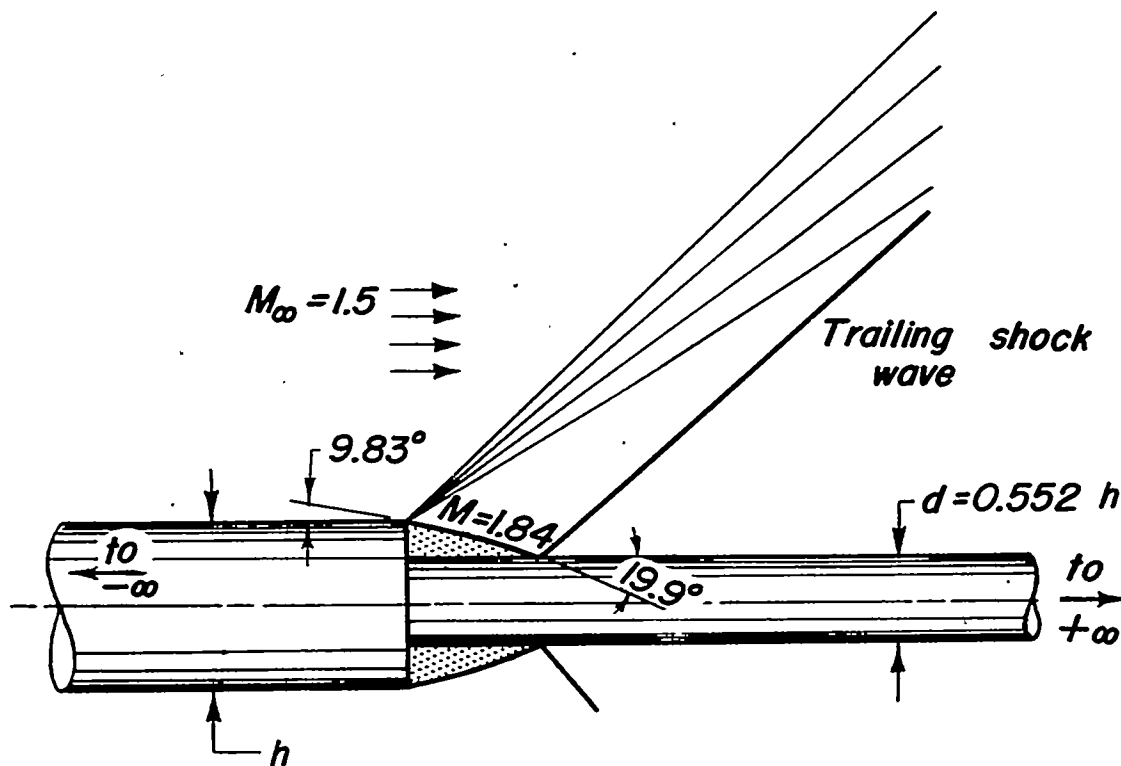
Figure 6. —Axially-symmetric semi-infinite body with rod attached.
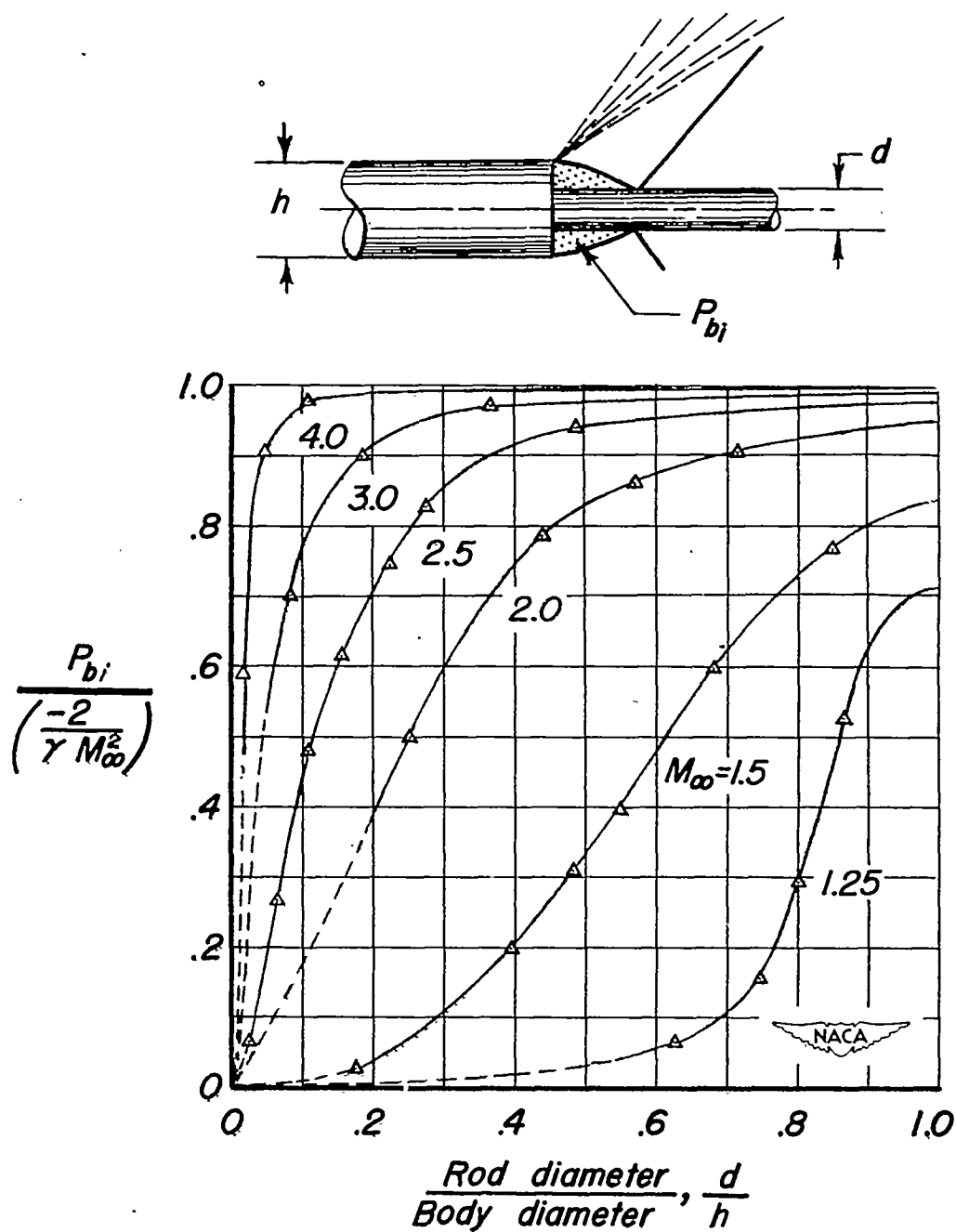
Figure 7. — Maximum base drag possible in an inviscid axially—symmetric flow.

(a) With rod attached.

(b) Without rod attached.

Figure 8. — Inviscid flow over a finite axially—symmetric body.
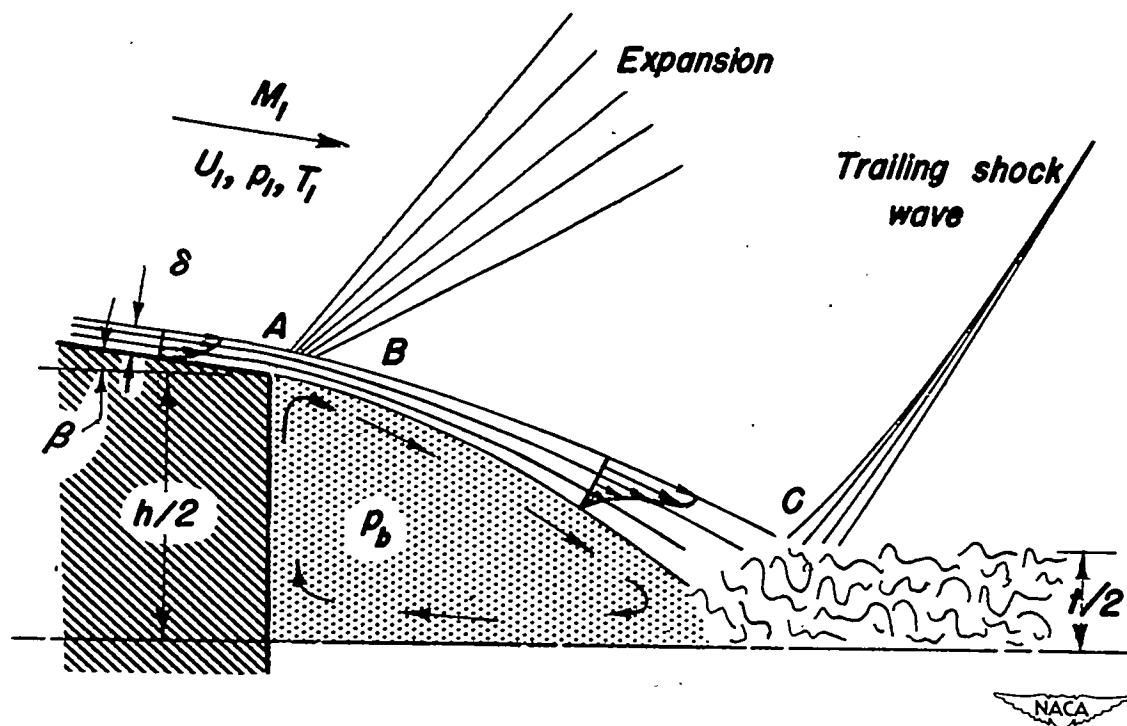
Figure 9. —Sketch of the viscous fluid flow in the neighborhood of the base.
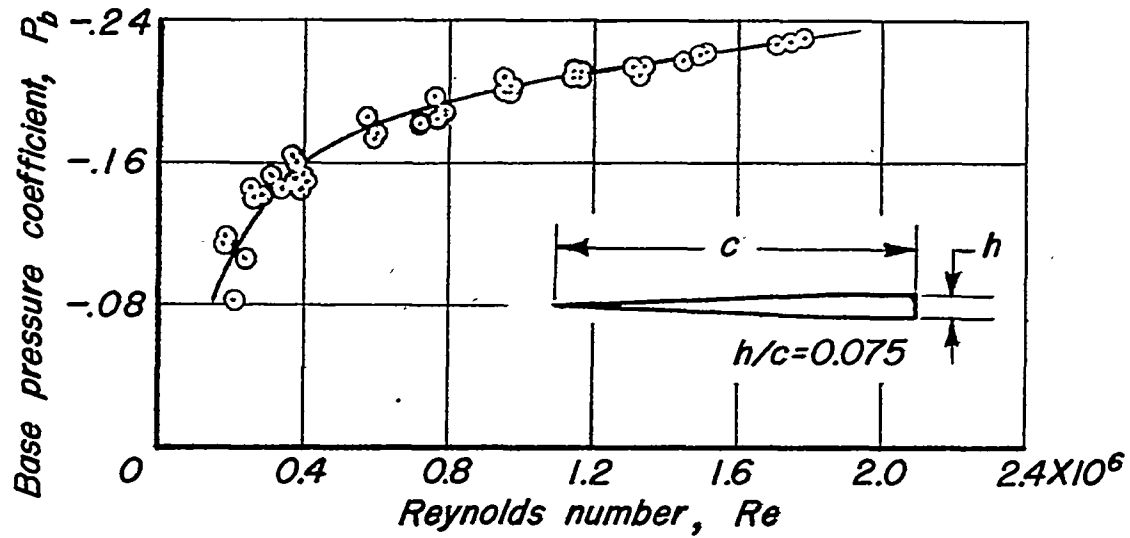
(a) Base pressure as a function of Reynolds number.
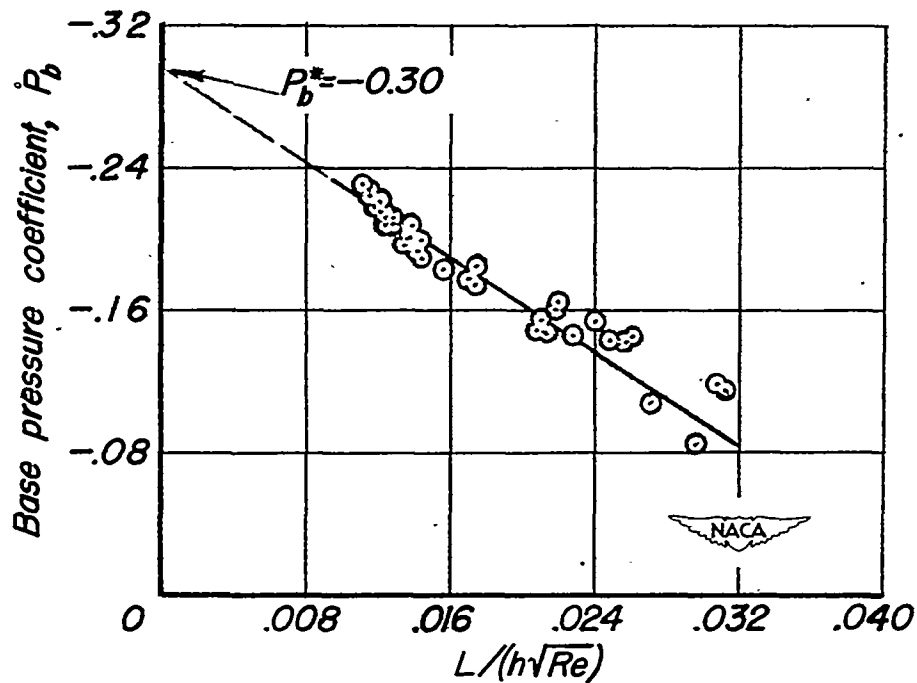
(b) Base pressure as a function of $L/h\sqrt{Re}$.

Figure 10. — Measured base pressure on a finite—span wing; $M_\infty = 2.0$, ratio of wing span to base thickness = 40.
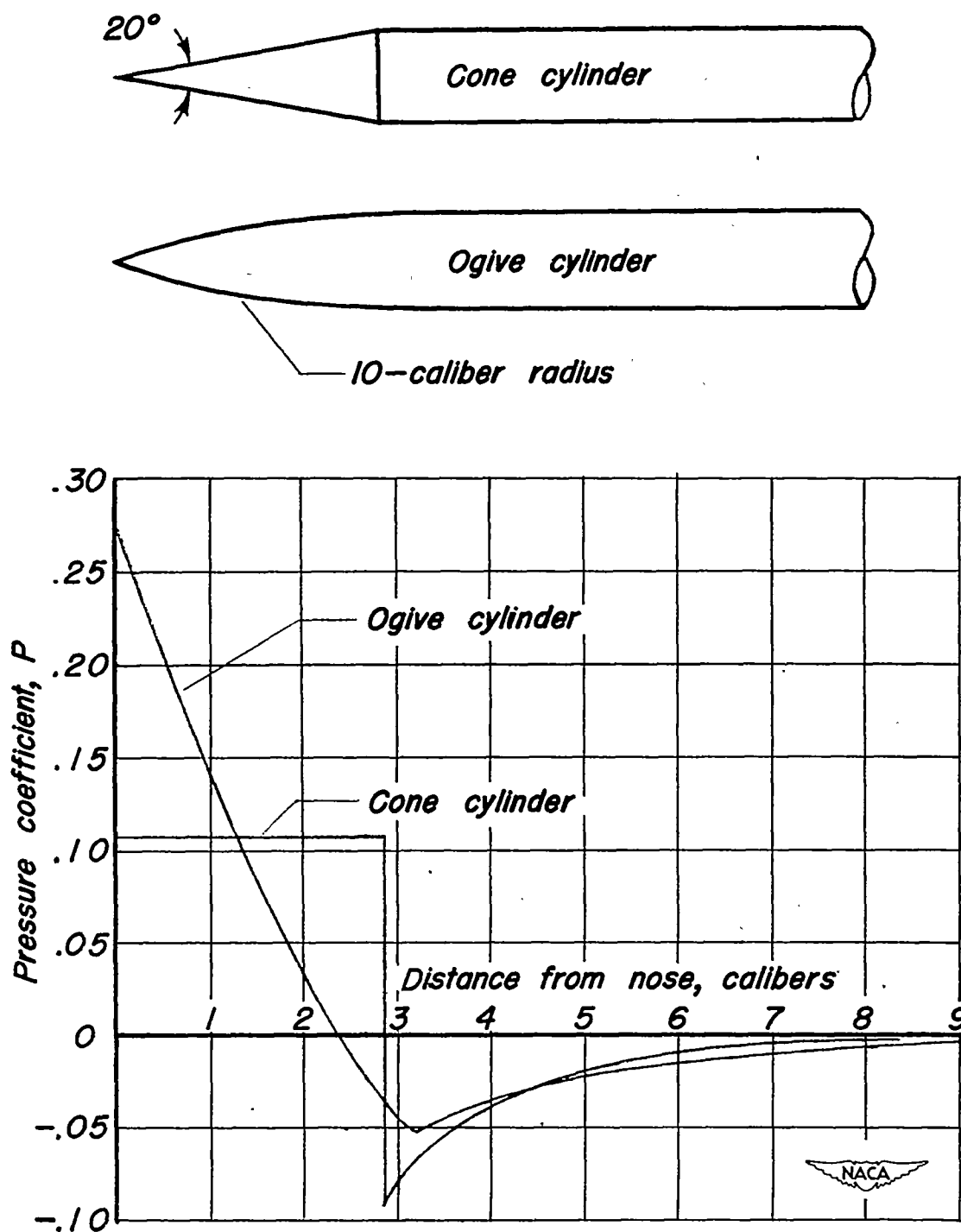
Figure II. — Typical pressure distribution as determined by the method of characteristics; $M_\infty = 2.0$.
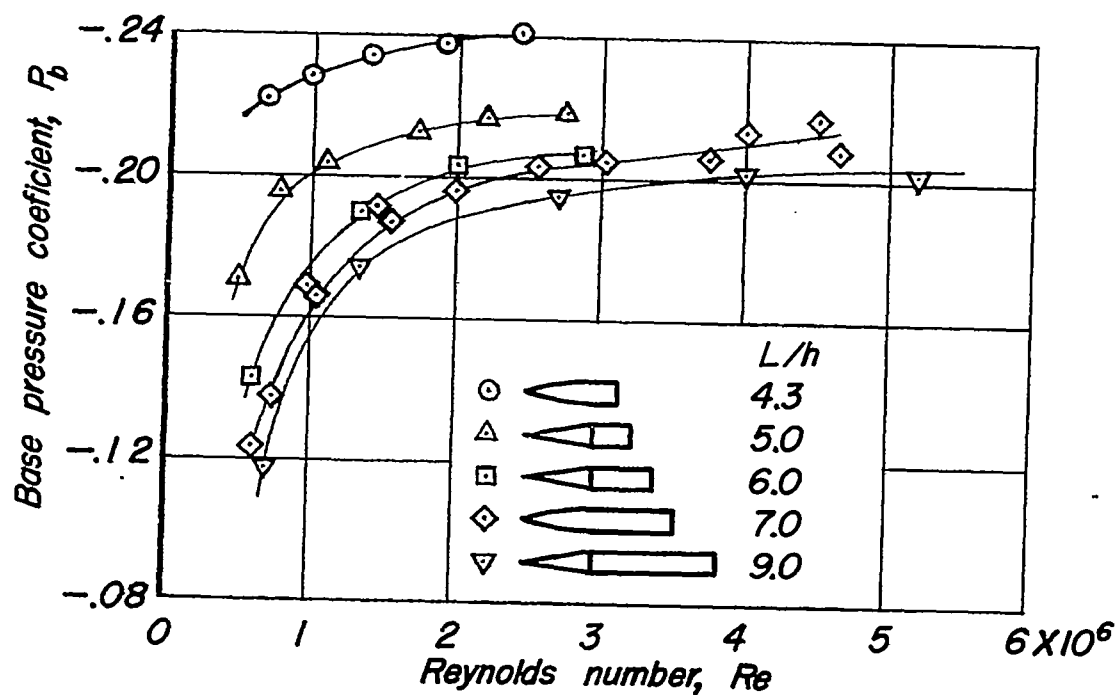
(a) Measured data.
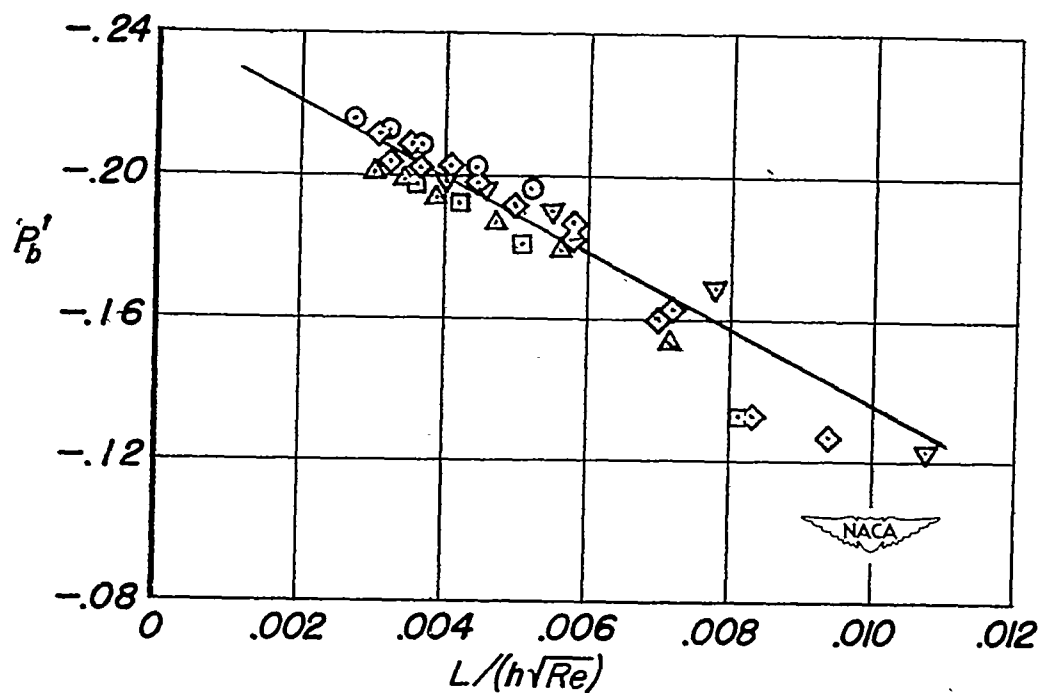
(b) Correlation of measured data.

Figure 12.—Measured and correlated base pressure data;
$M_\infty=1.53$, laminar boundary-layer flow.
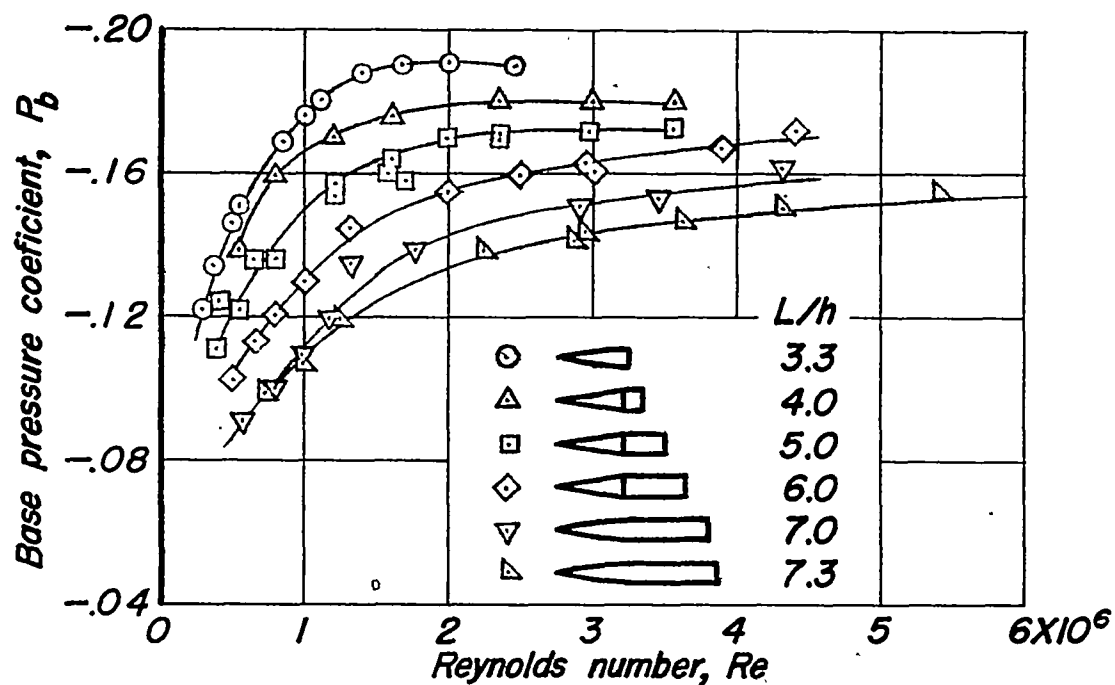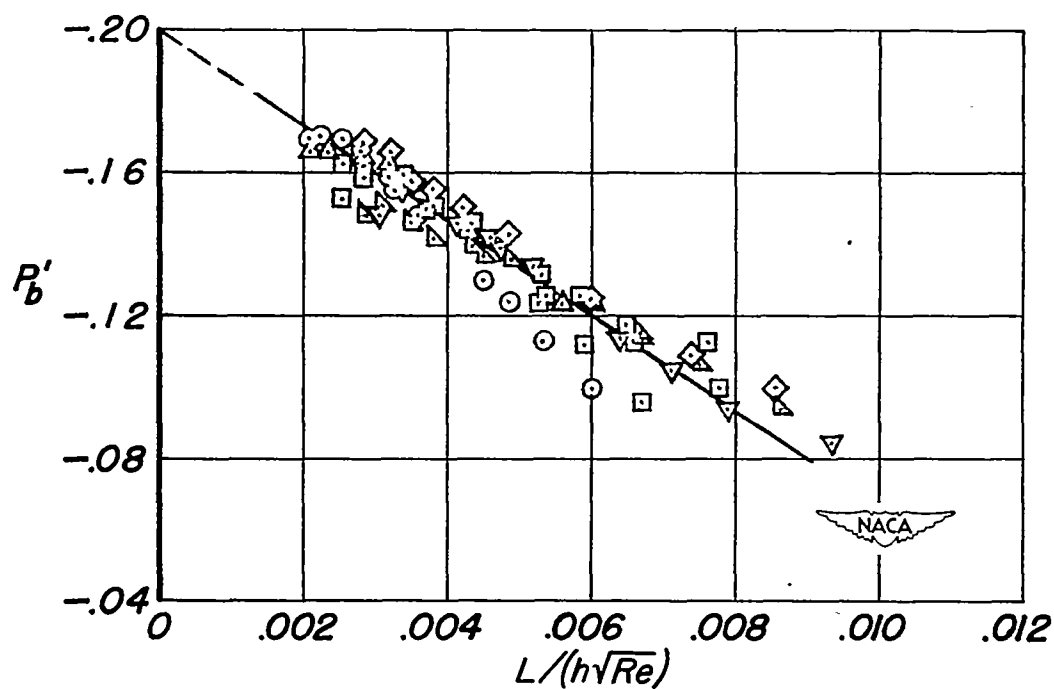
(a) Measured data.

(b) Correlation of measured data.

Figure 13. —Measured and correlated base pressure data; M_∞=2.0, laminar boundary-layer flow.
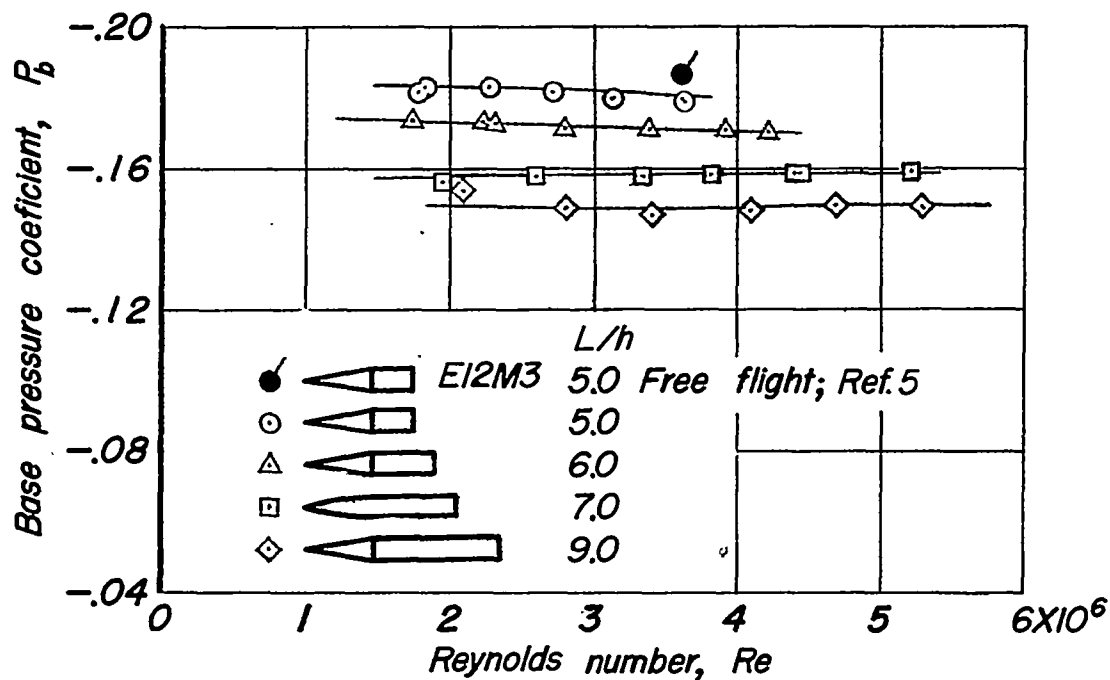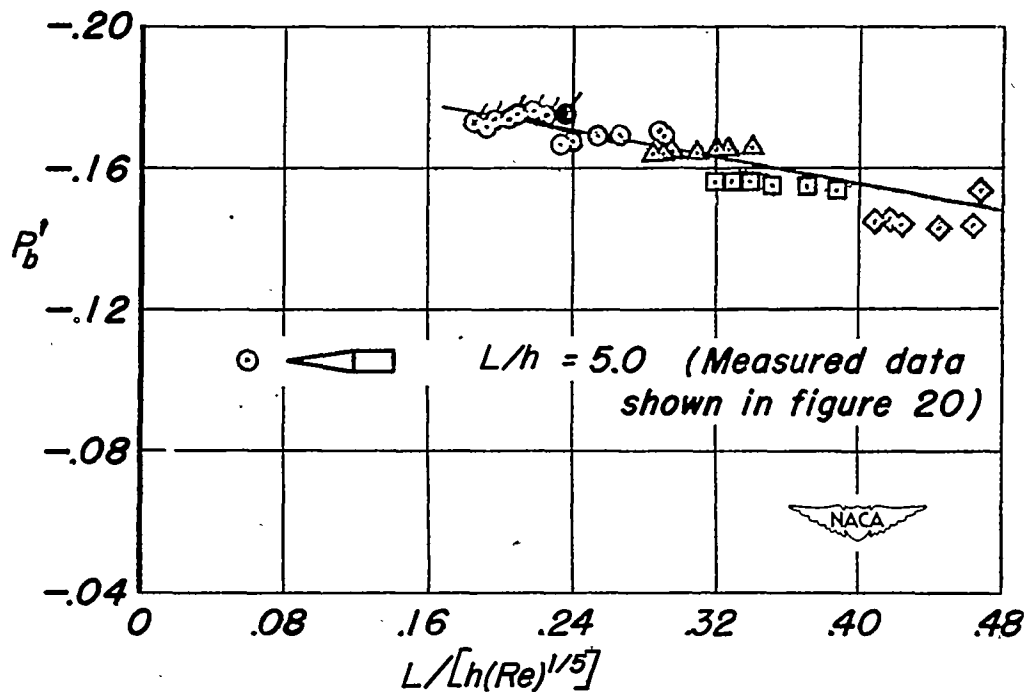
(a) Measured data.

(b) Correlation of measured data.

Figure 14. —Measured and correlated base pressure data;
$M_\infty = 1.5$, turbulent boundary—layer flow.

(a) Measured data.

(b) Correlation of measured data.
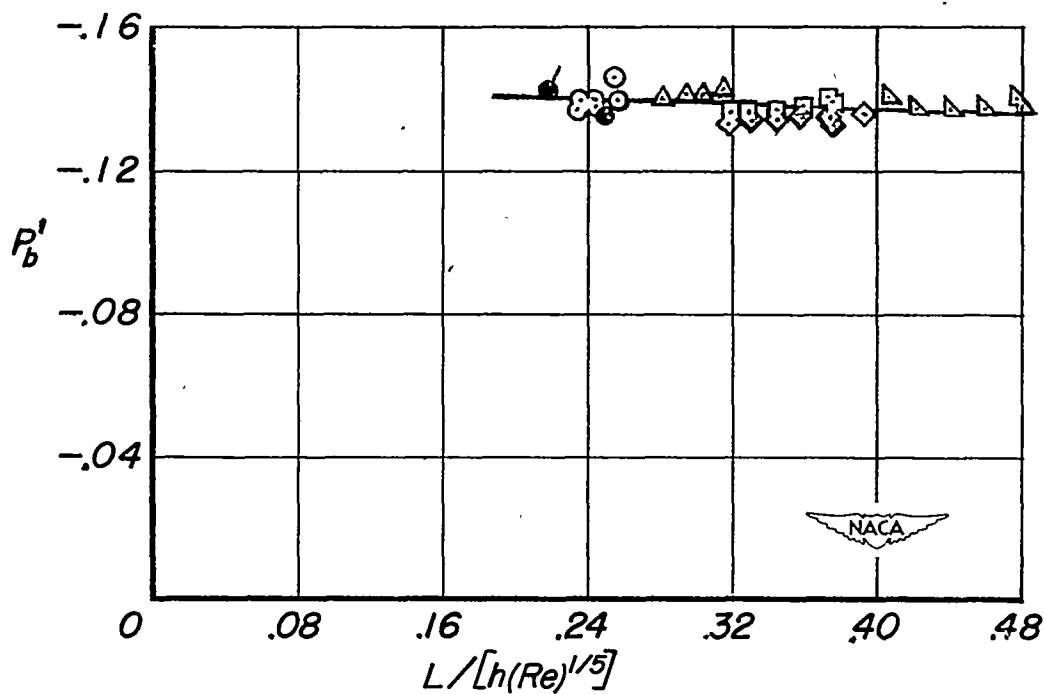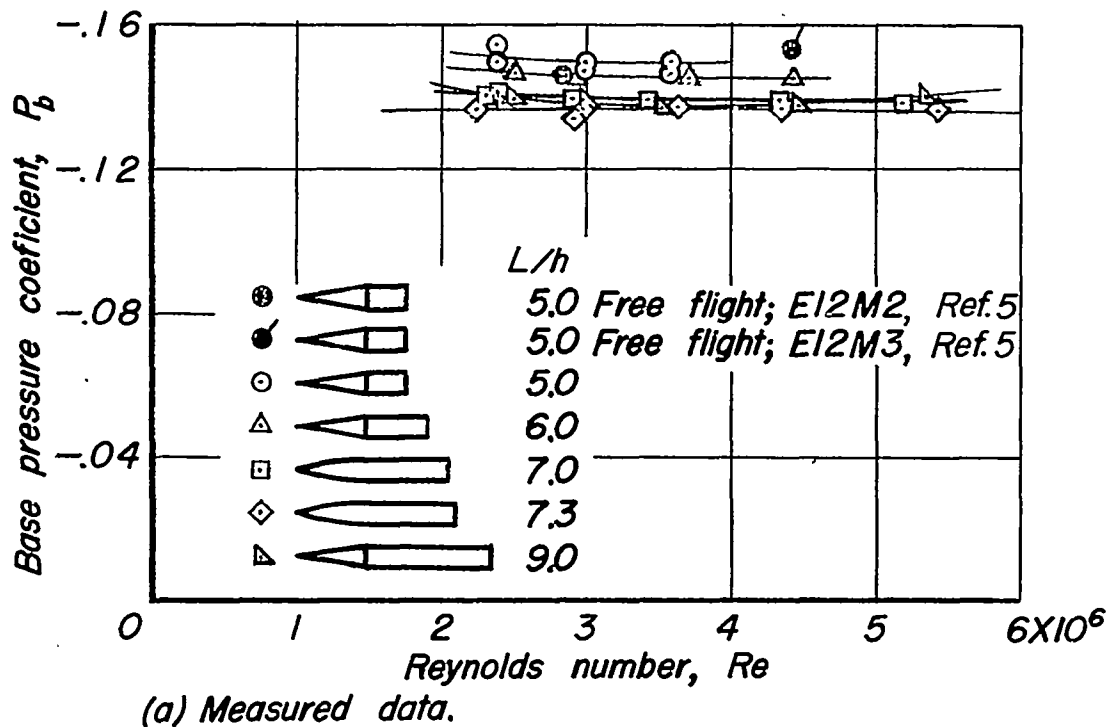
Figure 15.— Measured and correlated base pressure data; $M_\infty = 2.0$, turbulent boundary-layer flow.
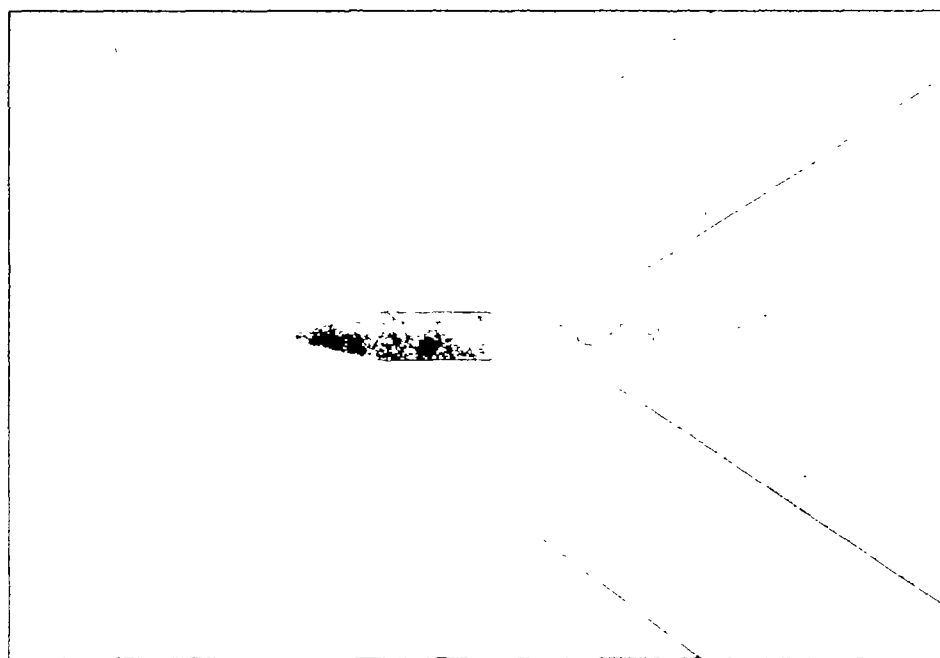
(a) $M_\infty = 1.73$, laminar.
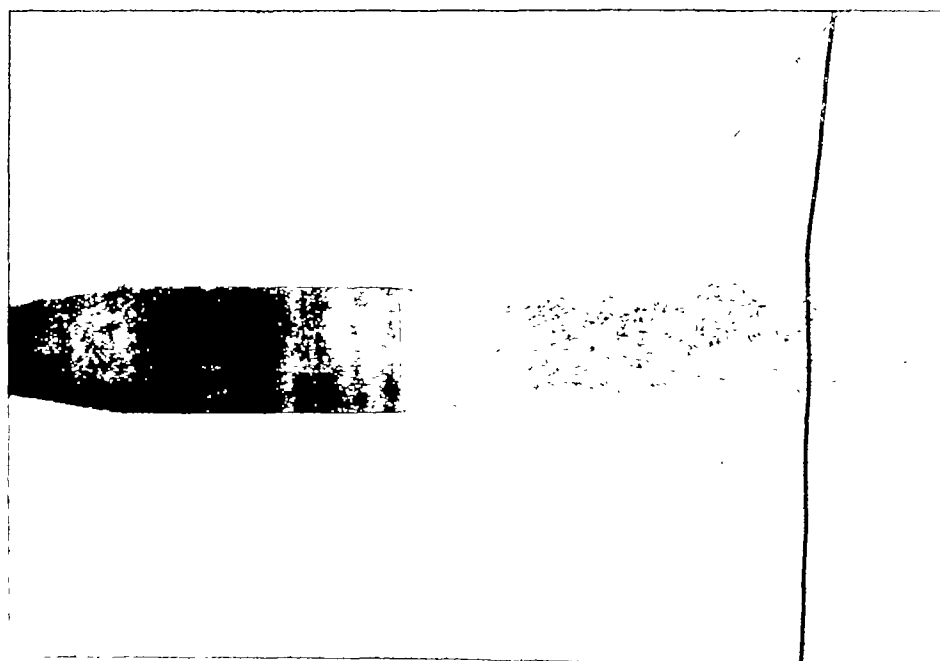
(b) $M_\infty = 1.28$, turbulent.

A-14621

Figure 16. —Shadowgraphs of projectiles in flight. (Courtesy Ballistic Research Laboratories, Aberdeen, Md.).
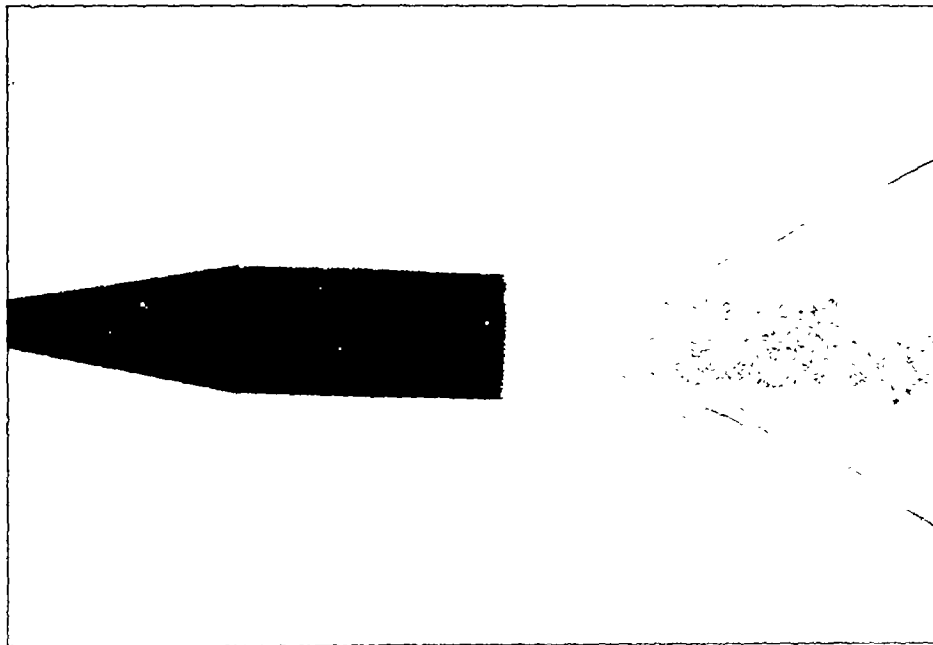
(c) $M_\infty = 1.88$, turbulent.
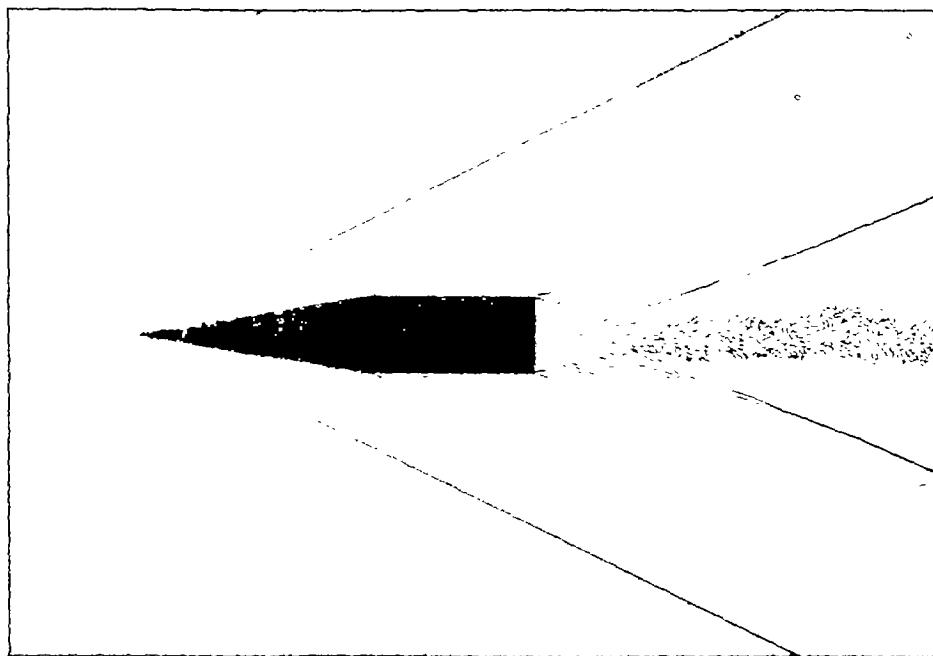
(d) $M_\infty = 2.33$ turbulent.

NACA
A-14622

Figure 16. —Continued.

(e) $M_{\infty} = 3.64$, turbulent.

A-14623
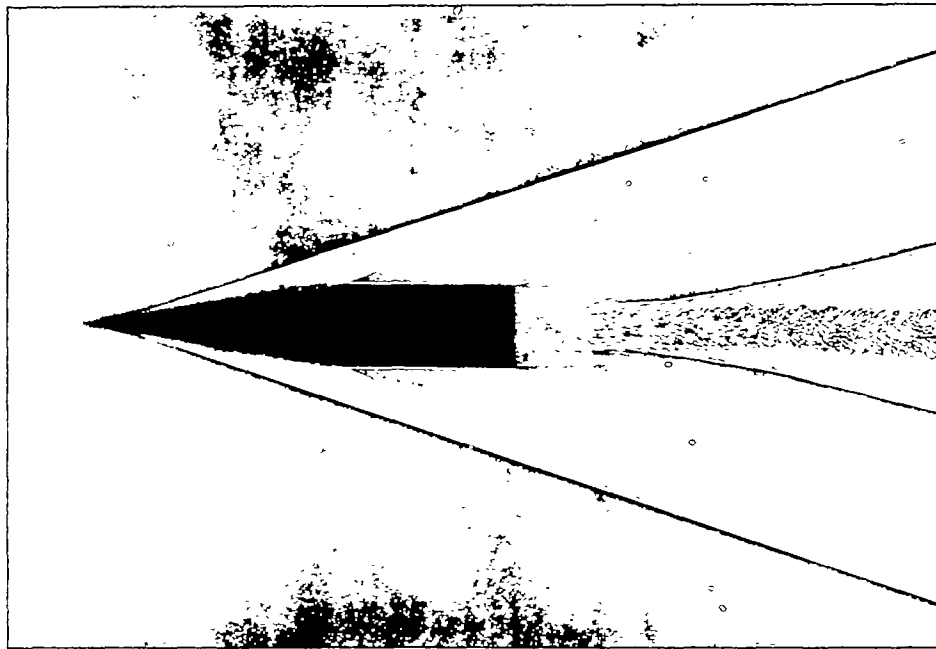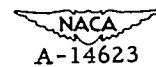
Figure 16.—Concluded.
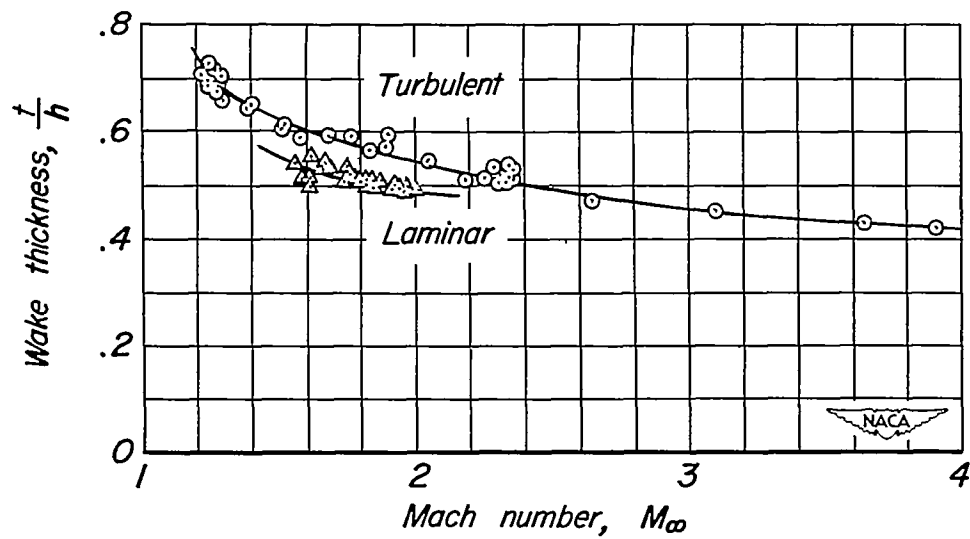
Figure 17.—Wake thickness as a function of Mach number (determined from shadowgraphs of the Ballistic Research Laboratories, Aberdeen, Md.).
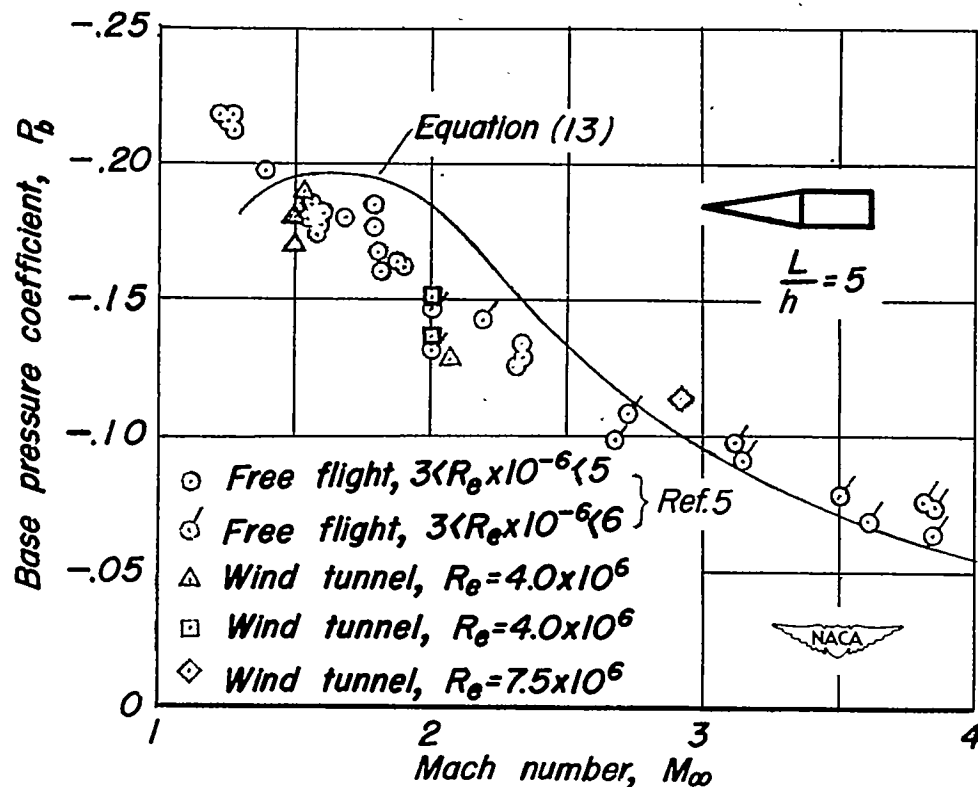
Figure 18.—Base pressure coefficient as a function of Mach number; turbulent boundary-layer flow.
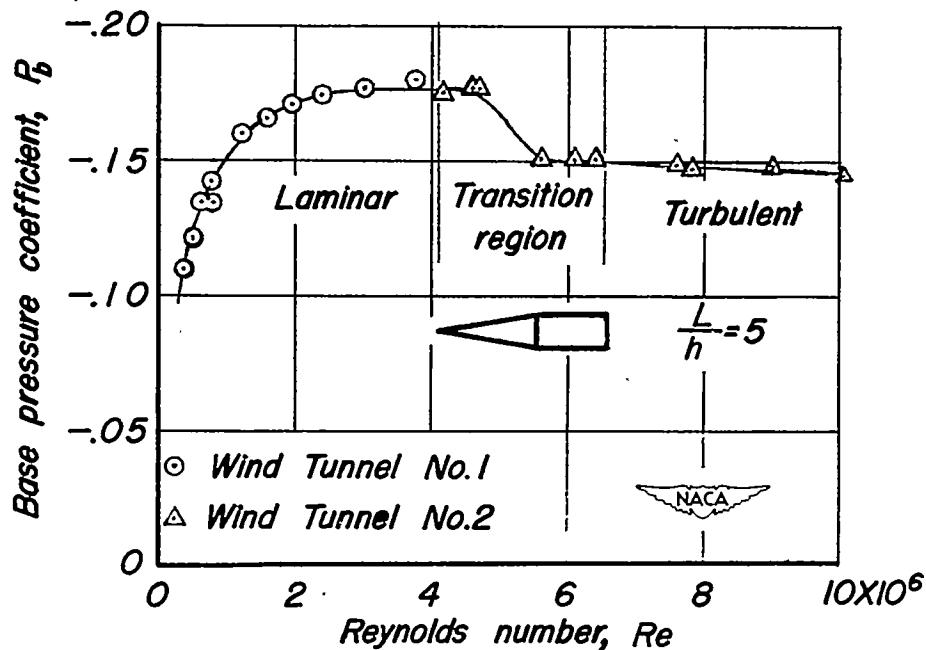
Figure 19.—Variation of base pressure coefficient with Reynolds number for natural transition; M_∞=2.0.
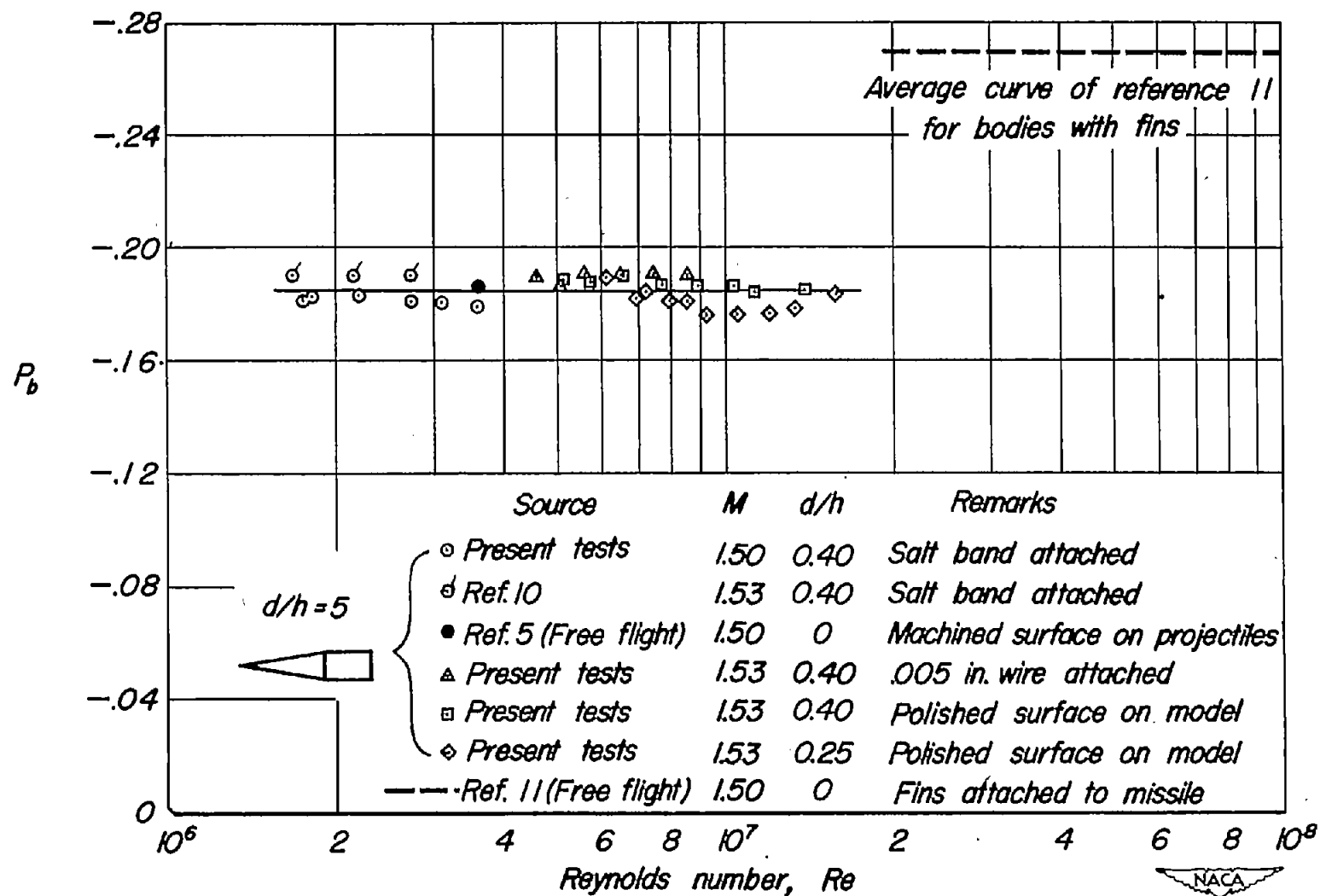
Figure 20. —Variation of base pressure with Reynolds number for turbulent boundary—layer flow; $M_\infty = 1.5$.
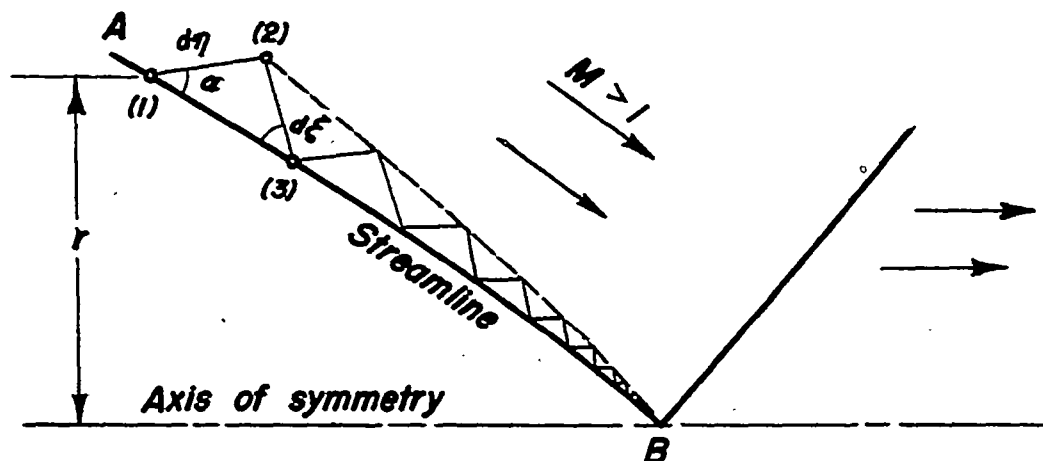
(a) Assumed flow in the physical plane.
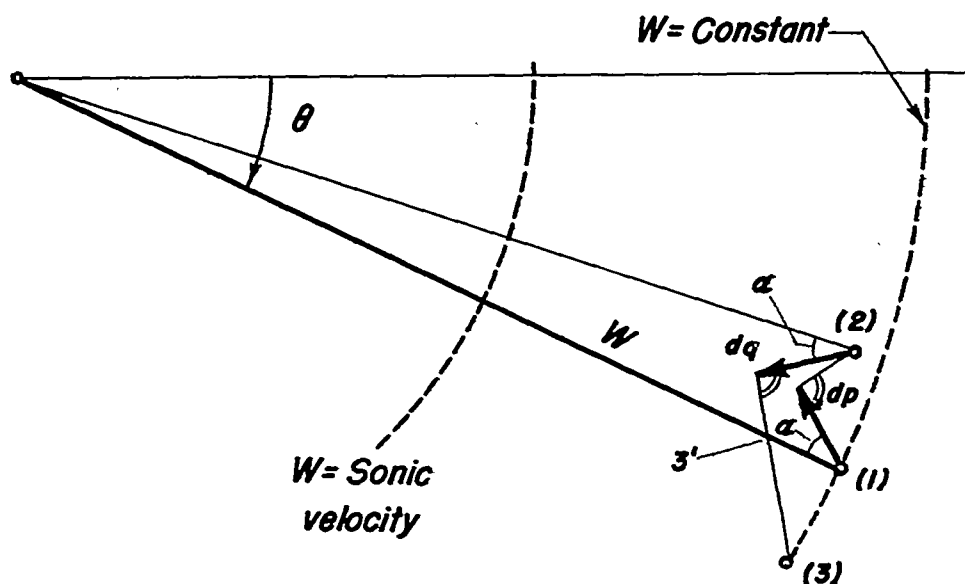
(b) Increments in hodograph plane corresponding to figure 21a.

Figure 21. —Characteristics construction for flows converging to the axis.
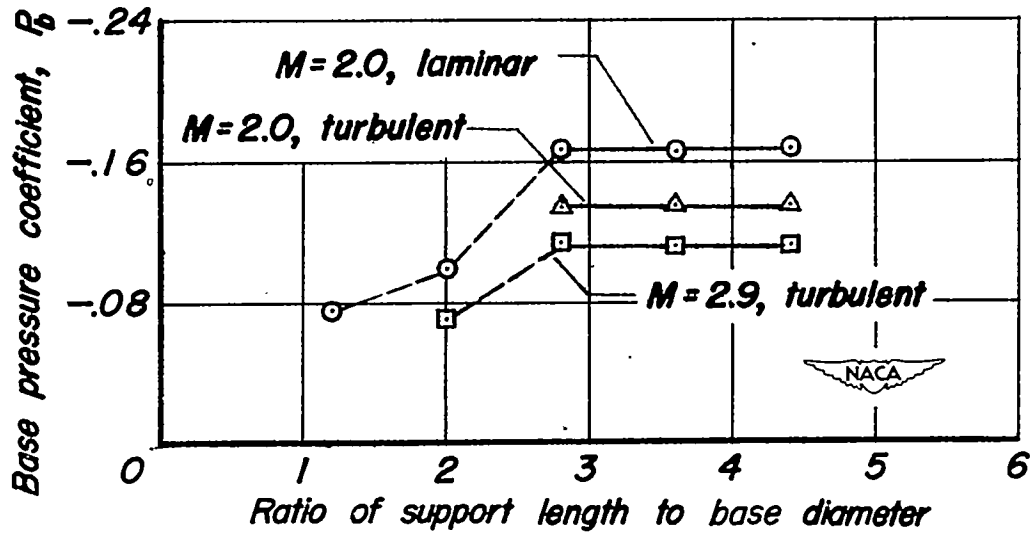
Figure 22.—Effect of support length on base pressure; d/h =0.3.
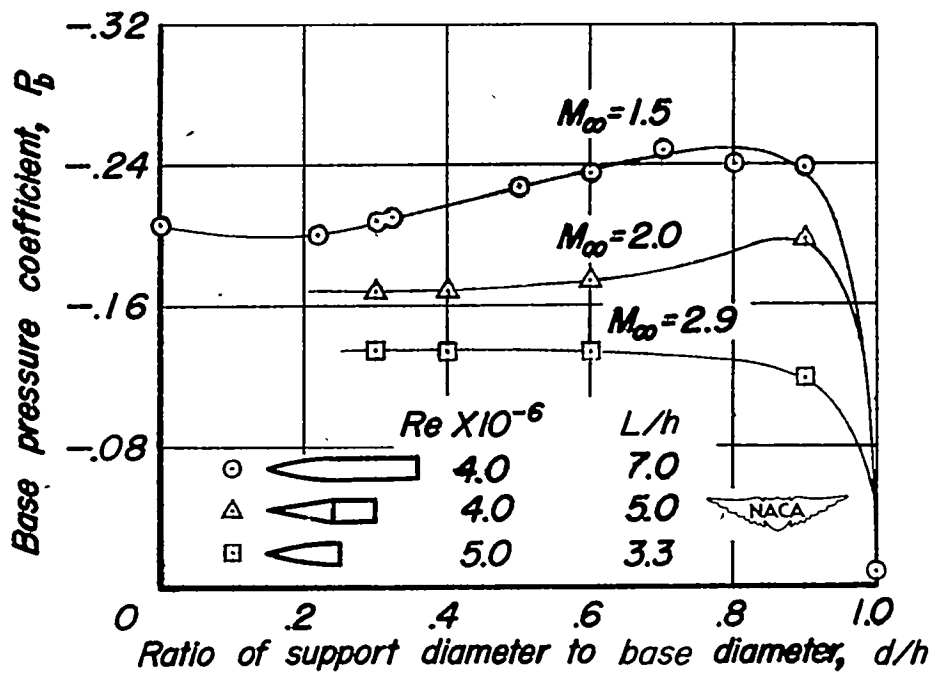
(a) Laminar.

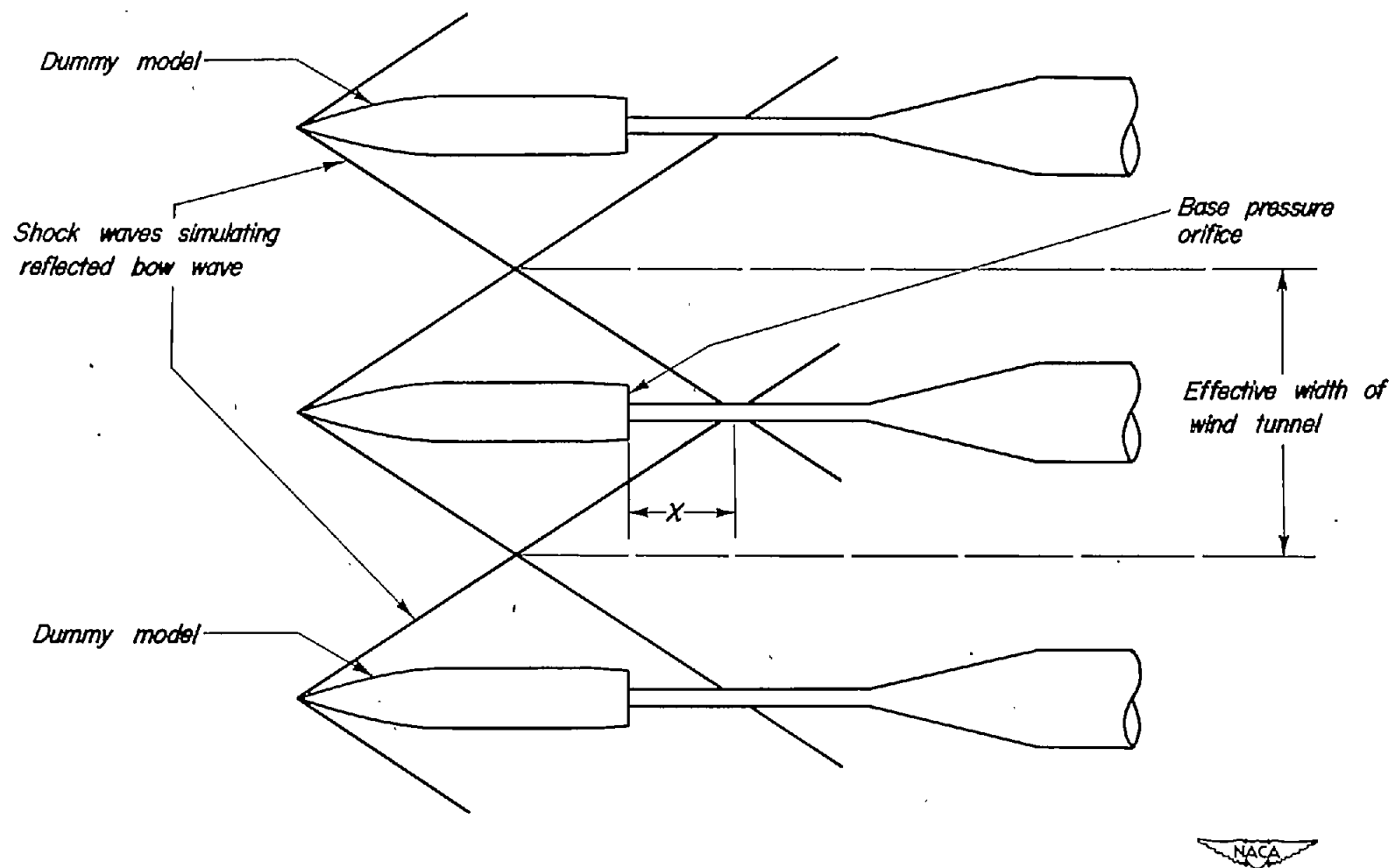Figure 23. —Effect of support diameter on base pressure.

Ratio of support diameter to base diameter, d/h

(b) Turbulent.

Figure 23. —Concluded.

Dummy model

Shock waves simulating
reflected bow wave

Base pressure
orifice

Effective width of
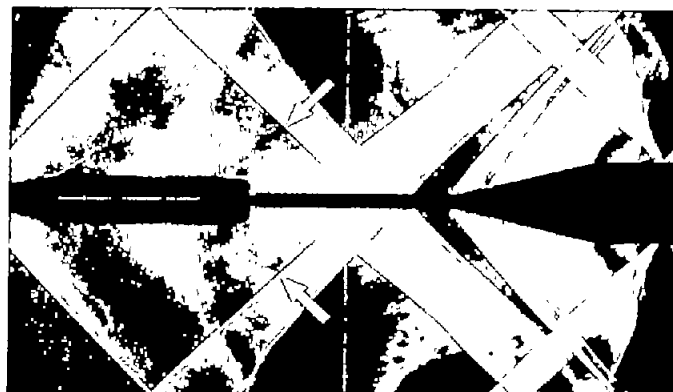wind tunnel

$\leftarrow X \rightarrow$

Dummy model

NACA
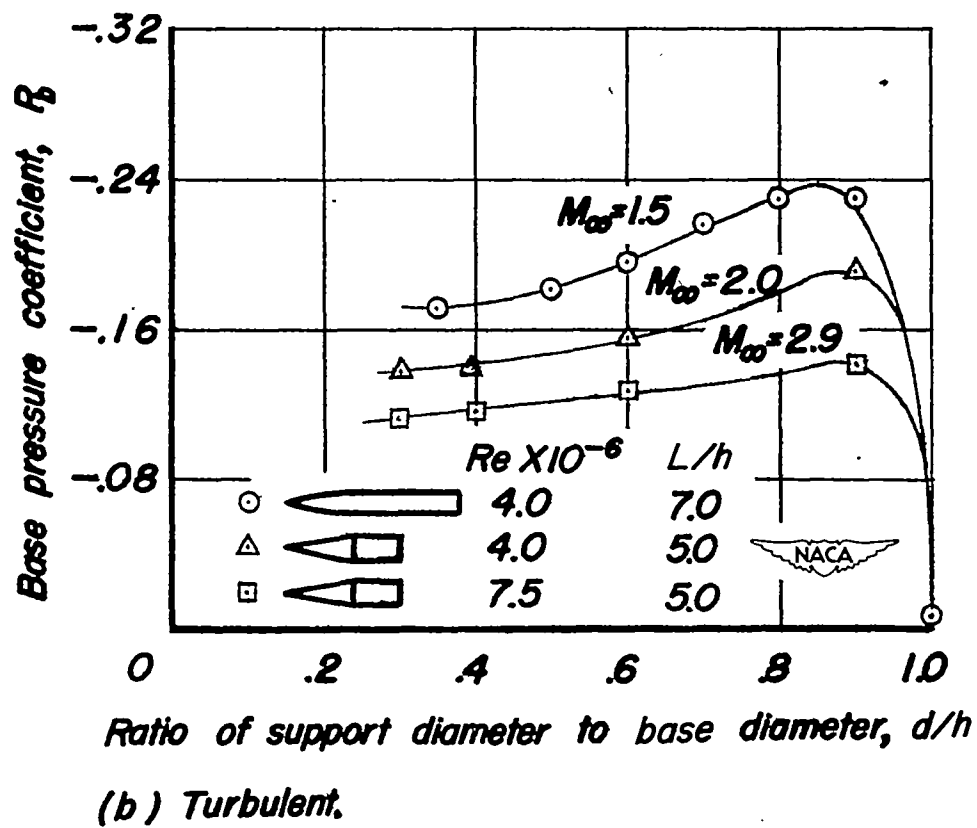
Figure 24. —Sketch of test setup used for determining the effect of a reflected bow wave on base pressure.
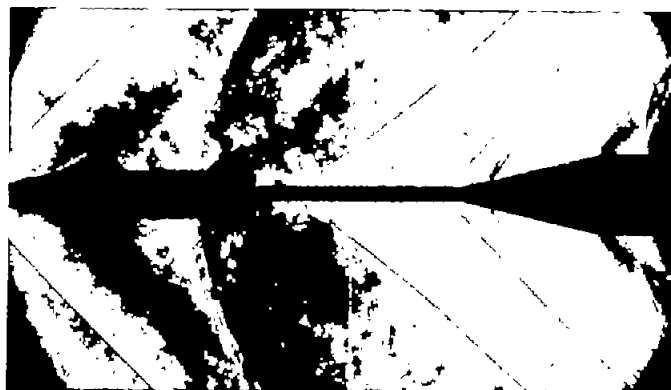
(a) Flow without dummy models.
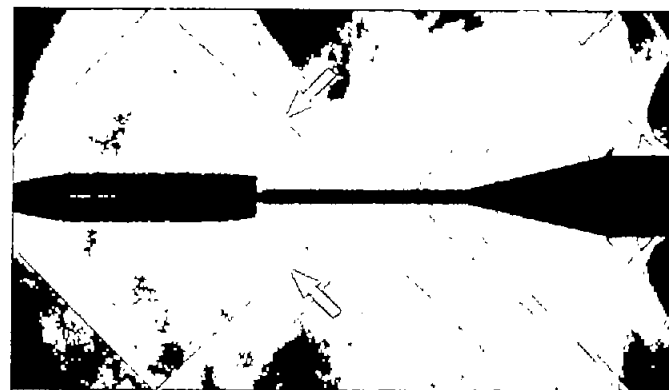
(b) Re=0.9X10⁶; X=2.5h .

(c) Re=2.7X10⁶; X=2.5h .

(d) Re=2.7X10⁶; X=0.9h .

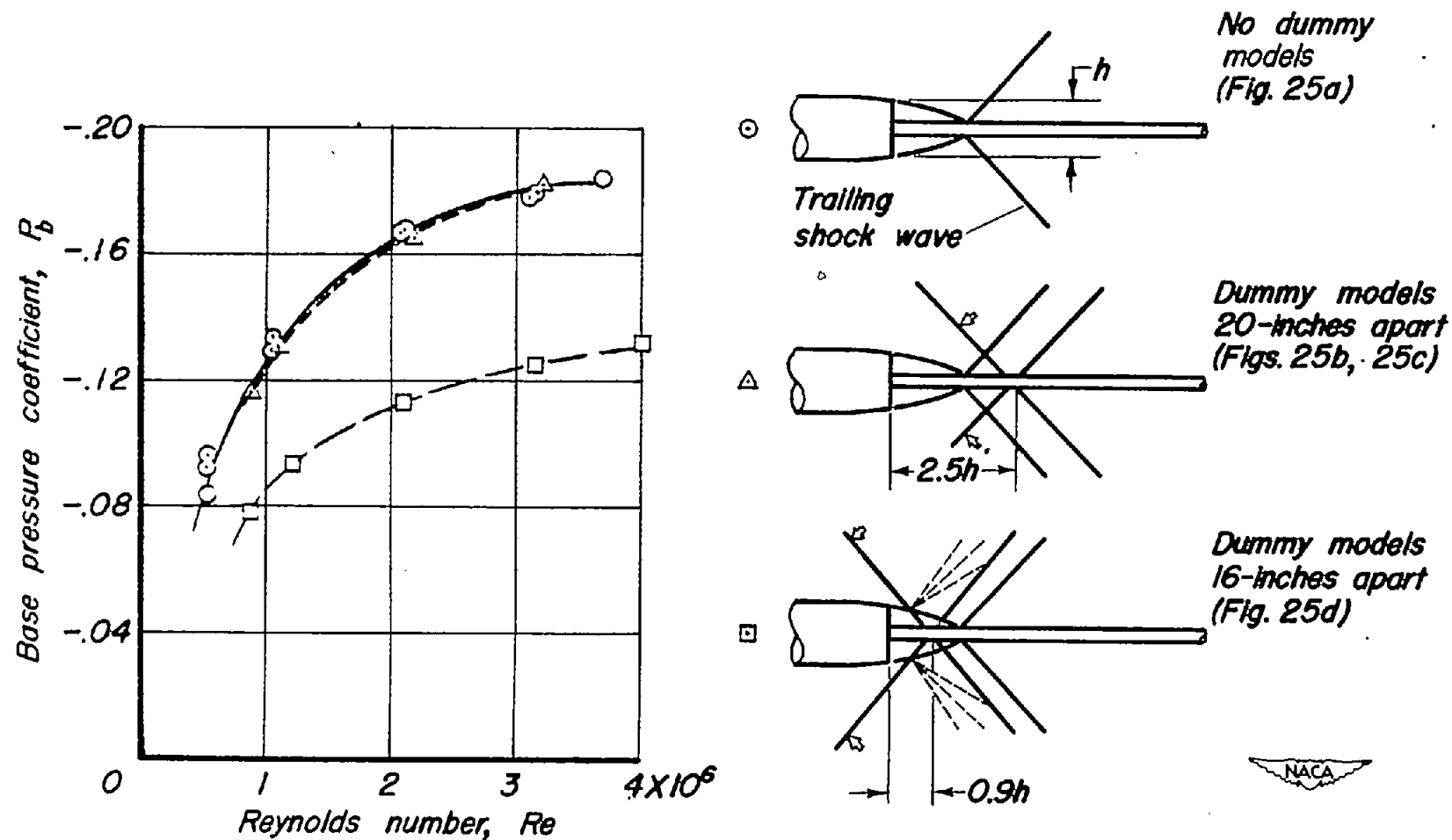Figure 25. — Schlieren photographs for various positions of intersection of the shock waves simulating reflected bow waves; M=1.53.

Figure 26. —Effect of reflected bow waves on base pressure; M=1.53.